



**HAL**  
open science

## Activating ATF6 in spinal muscular atrophy promotes SMN expression and motor neuron survival through the IRE1 $\alpha$ -XBP1 pathway

Domenico d'Amico, Olivier Biondi, Camille Januel, Cynthia Bezier, Delphine Sapaly, Zoé Clerc, Mirella El Khoury, Venkat Krishnan Sundaram, Léo Houdebine, Thibaut Josse, et al.

### ► To cite this version:

Domenico d'Amico, Olivier Biondi, Camille Januel, Cynthia Bezier, Delphine Sapaly, et al.. Activating ATF6 in spinal muscular atrophy promotes SMN expression and motor neuron survival through the IRE1 $\alpha$ -XBP1 pathway. *Neuropathology and Applied Neurobiology*, 2022, 48 (5), pp.e12816. 10.1111/nan.12816 . inserm-04385529

**HAL Id: inserm-04385529**

**<https://inserm.hal.science/inserm-04385529>**

Submitted on 10 Jan 2024

**HAL** is a multi-disciplinary open access archive for the deposit and dissemination of scientific research documents, whether they are published or not. The documents may come from teaching and research institutions in France or abroad, or from public or private research centers.

L'archive ouverte pluridisciplinaire **HAL**, est destinée au dépôt et à la diffusion de documents scientifiques de niveau recherche, publiés ou non, émanant des établissements d'enseignement et de recherche français ou étrangers, des laboratoires publics ou privés.



Distributed under a Creative Commons Attribution 4.0 International License

# Activating ATF6 in spinal muscular atrophy promotes SMN expression and motor neuron survival through the IRE1 $\alpha$ -XBP1 pathway

Domenico D'Amico<sup>1</sup> | Olivier Biondi<sup>1</sup> | Camille Januel<sup>2</sup> | Cynthia Bezier<sup>1,3</sup> |  
Delphine Sapaly<sup>1</sup> | Zoé Clerc<sup>1</sup> | Mirella El Khoury<sup>1</sup> | Venkat Krishnan Sundaram<sup>1</sup> |  
Léo Houdebine<sup>1</sup> | Thibaut Josse<sup>4</sup> | Bruno Della Gaspera<sup>1</sup> | Cécile Martinat<sup>2</sup>  |  
Charbel Massaad<sup>1</sup> | Laure Weill<sup>1</sup>  | Frédéric Charbonnier<sup>1</sup>

<sup>1</sup>Université Paris cité and Inserm UMR\_S1124, Paris, France

<sup>2</sup>Université d'Evry-Val-d'Essonne and Inserm UMR 861, I-STEM, AFM, Corbeil-Essonnes, France

<sup>3</sup>Biophytis, Sorbonne Université, Paris, France

<sup>4</sup>Université de Tours and CNRS UMR 7261, Institut de Recherche sur la Biologie de l'Insecte, Tours, France

## Correspondence

Frédéric Charbonnier and Laure Weill, Université Paris cité and Inserm UMR\_S1124, 45 rue des Saints-Pères, F-75270 Paris Cedex 06, France.

Email: [frederic.charbonnier@u-paris.fr](mailto:frederic.charbonnier@u-paris.fr); [laure.weill@u-paris.fr](mailto:laure.weill@u-paris.fr)

## Abstract

**Aim:** Spinal muscular atrophy (SMA) is a neuromuscular disease caused by survival of motor neuron (SMN) deficiency that induces motor neuron (MN) degeneration and severe muscular atrophy. Gene therapies that increase SMN have proven their efficacy but not for all patients. Here, we explored the unfolded protein response (UPR) status in SMA pathology and explored whether UPR modulation could be beneficial for SMA patients.

**Methods:** We analysed the expression and activation of key UPR proteins by RT-qPCR and by western blots in SMA patient iPSC-derived MNs and one SMA cell line in which SMN expression was re-established (rescue). We complemented this approach by using myoblast and fibroblast SMA patient cells and SMA mouse models of varying severities. Finally, we tested in vitro and in vivo the effect of IRE1 $\alpha$ /XBP1 pathway restoration on SMN expression and subsequent neuroprotection.

**Results:** We report that the IRE1 $\alpha$ /XBP1 branch of the unfolded protein response is disrupted in SMA, with a depletion of XBP1s irrespective of IRE1 $\alpha$  activation pattern. The overexpression of XBP1s in SMA fibroblasts proved to transcriptionally enhance SMN expression. Importantly, rebalancing XBP1s expression in severe SMA-like mice, induced SMN expression and spinal MN protection.

**Conclusions:** We have identified XBP1s depletion as a contributing factor in SMA pathogenesis, and the modulation of this transcription factor proves to be a plausible therapeutic avenue in the context of pharmacological interventions for patients.

## KEYWORDS

IRE1 $\alpha$ , neuroprotection, SMN, spinal muscular atrophy, unfolded protein response, XBP1

This is an open access article under the terms of the [Creative Commons Attribution-NonCommercial-NoDerivs](https://creativecommons.org/licenses/by-nc-nd/4.0/) License, which permits use and distribution in any medium, provided the original work is properly cited, the use is non-commercial and no modifications or adaptations are made.

© 2022 The Authors. *Neuropathology and Applied Neurobiology* published by John Wiley & Sons Ltd on behalf of British Neuropathological Society.

## INTRODUCTION

Spinal muscular atrophy (SMA) is a childhood neuromuscular disease caused by survival of motor neuron 1 (*SMN1*) gene mutation or deletion and subsequent protein depletion [1]. SMA induces motor-neuron (MN) degeneration leading to severe muscular atrophy and often to early death [2]. The severity of SMA is variable depending on the expression of *SMN2*, a gene copy of *SMN1*. Indeed, due to a polymorphism in exon-7, *SMN2* produces only a fraction of the full-length *SMN* mRNA leading to the production of a small amount of functional *SMN* protein [3]. Consequently, efforts to find a therapy for SMA have mainly focused on increasing full-length *SMN* expression in patients. Three therapies for SMA are available, based either on the promotion of exon-7 inclusion in *SMN2*-derived transcripts using specific Antisense Oligonucleotides [4–6] or the Ridisplam molecule [7], or on AAV-based *SMN1* gene replacement [8]. Although proven to alleviate SMA, these therapies do not constitute a cure for SMA and are not efficient or applicable for all patients [6, 9–12]. Furthermore, the existence of AAV immunoreactivity limits *SMN* gene replacement by AAV [13]. Thus, novel therapeutic approaches are needed to increase the number of available treatment options for all patients, including original combination therapies.

We previously reported in several severe SMA mouse models, that increasing MN activity, either physiologically using physical exercise [14] or pharmacologically using agonists of NMDA receptors [15], promotes MN survival likely through *SMN* expression-promoting mechanisms that remain to be further investigated. Among these mechanisms, NMDA-receptor activation could trigger the unfolded protein response (UPR) [16].

The UPR is an adaptive system activated when unfolded or misfolded proteins accumulate in the lumen of the endoplasmic reticulum (ER). UPR is expected to restore normal cell function primarily by halting general translation, followed by degrading unfolded proteins and subsequently inducing the expression of chaperones involved in protein folding, such as the binding immunoglobulin protein BiP/GRP78 or protein disulfide isomerases (PDIs). Thus, the UPR system restores the balance between folding capacity and demand through the activation of three branch-specific transcription factors, that is, XBP1, ATF4 or ATF6, respectively, activated by inositol-requiring enzyme 1  $\alpha$  (IRE1 $\alpha$ ), PKR-like ER kinase (PERK) and ATF6 [17] (Figure 1). Under normal conditions, IRE1 $\alpha$  binds BiP/GRP78 in an inactive complex. When unfolded proteins accumulate in the ER, BiP/GRP78 dissociates from IRE1 $\alpha$ , which then undergoes homodimerization and *trans*-autophosphorylation [18]. IRE1 $\alpha$  autophosphorylation results in the activation of its endoribonuclease domain [19] that catalyses 26 nucleotide excision in unspliced *XBP1* (*XBP1u*) mRNA [20]. This *XBP1* mRNA splicing, which unconventionally occurs in the cytoplasm, generates the spliced *XBP1* (*XBP1s*) with a new open reading frame encoding the active form of XBP1 (*XBP1s*). The latter can enter into the nucleus, bind to cAMP response element (CRE) and activate transcription of its target genes, such as BiP/GRP78 or PDIs [20] (Figure 1). If this adaptive mechanism fails, the UPR switches to a pro-apoptotic mode, notably through the

### Key points

- IRE1 $\alpha$ /XBP1 branch of the unfolded protein response is disrupted in SMA, with a depletion of XBP1s irrespective of IRE1 $\alpha$  activation pattern.
- Restoration of XBP1s by overexpression in SMA fibroblasts proved to transcriptionally enhance *SMN* expression.
- ATF6 Activation led to rebalance XBP1s expression in severe SMA-like mice, inducing *SMN* expression and spinal MN protection.

activation of the regulated IRE1 $\alpha$ -dependent decay of mRNA (RIDD) [21] or the induction of CCAAT/enhancer binding protein (C/EBP) homologous protein (CHOP), both resulting in the activation of an apoptosis signal-regulating kinase 1 (ASK1)-dependent signalling pathway [22].

Interestingly, using MNs derived from the severe-type patient induced pluripotent stem cell (iPSC) and a mouse model of severe type SMA, Rubin's laboratory reported that activated UPR promoted SMA MN death and that *in vivo* inhibition of UPR increased SMA MN survival [23]. However, these data were unconfirmed by a follow-up study also using also SMA iPSC-derived MNs [24]. This apparent discrepancy prompted us to explore the UPR status in two different cell lines of SMA patient iPSC-derived MNs and one SMA cell line in which *SMN* was re-expressed (rescue). We complemented this *in vitro* study by using myoblast and fibroblast SMA patient cells. Finally, we studied the spinal cord from different mouse models with varying disease severity. Our results suggest that the IRE1 $\alpha$ /XBP1 branch of the UPR is altered in SMA, with an overactivation of IRE1 $\alpha$  that is unexpectedly associated with a decrease in XBP1s expression. Importantly, XBP1s restoration promotes *SMN* expression *in vitro* and *in vivo* and MN survival in the spinal cord of severe SMA-like mice.

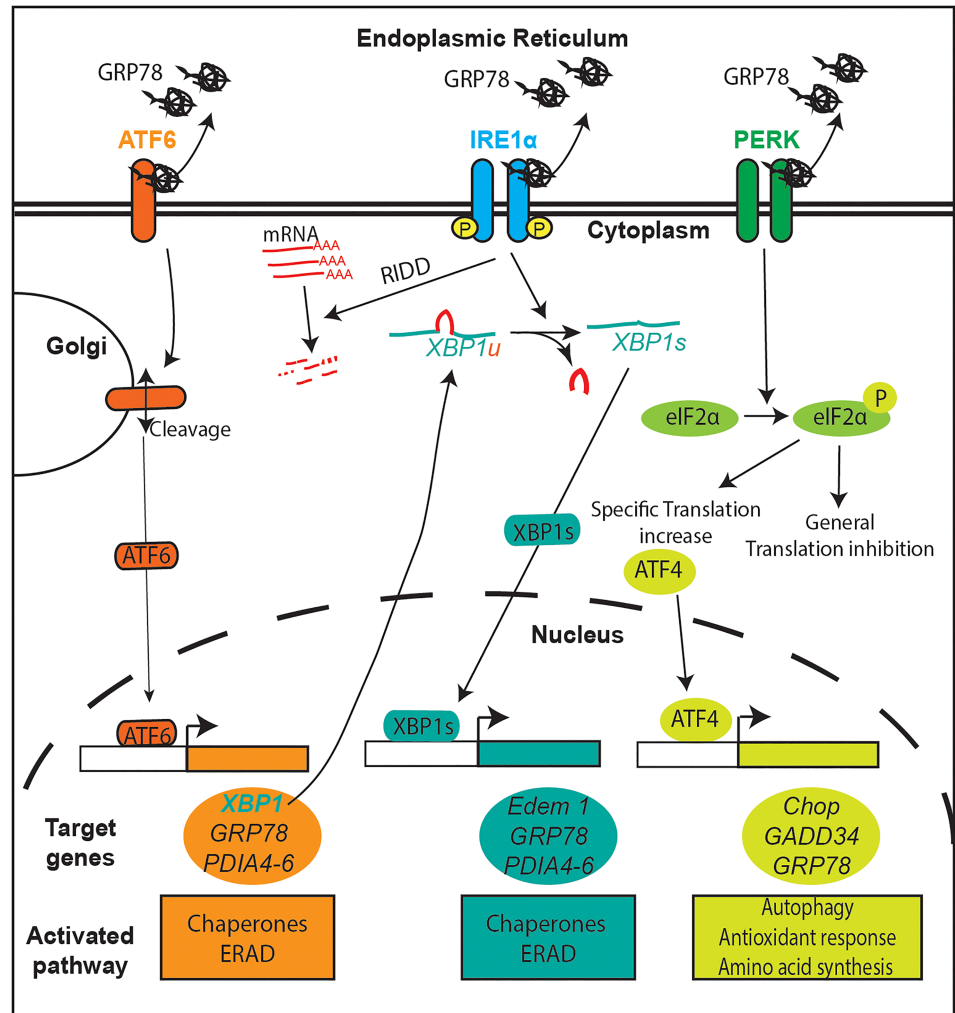
## MATERIALS AND METHODS

See Supporting Information for detailed descriptions.

### hiPSC-derived motor neurons

hiPSC were generated by reprogramming Coriell Biorepository patient fibroblasts as previously described [25]. Two independent control hiPSC and 2 SMA hiPSC were generated from fibroblast lines (Figure S1). An isogenic control SMA line was obtained from one SMA hiPSC line in which a plasmid encoding *SMN* (pEF1aFlagbiotagSMN-PGKpuro, kindly gift of H. Wichterle and S. Nedelec) was stably transfected (Rescue). Informed consent was obtained from all the patients included in this study, complying with the ethical guidelines of the

**FIGURE 1** Overview of UPR pathway in response to ER stress. Upon accumulation of misfolded proteins in the ER, GRP78 dissociates from the three ER stress sensors: IRE1 $\alpha$ , PERK and ATF6. This leads to the activation of ATF6 by cleavage and of IRE1 $\alpha$  and PERK by autophosphorylation. Once activated, ATF6 translocates in the nucleus and activates the transcription of its target genes, one of whom is *XBP1* gene. The transcript of this last gene is *XBP1u* that encodes an unstable protein. IRE1 $\alpha$  induces the unconventional splicing of *XBP1u* mRNA and produces *XBP1s* mRNA that encodes the active XBP1s transcription factor of this branch. Finally, PERK, through eIF2 $\alpha$  phosphorylation, increases the translation of the transcription factor ATF4 and inhibits the general translation. Thus, the activation of these three transcription factors induces the transcription of genes encoding chaperones and the ERAD system (ATF6, XBP1s), and autophagy and antioxidant responses (ATF4), allowing to restore the ER homeostasis, enhance protein folding and clear the misfolded proteins



institutions and with the legislation requirements of the country of origin. Experimental protocols were approved by the French Ministry of Health: A02599-48. For differentiation of spinal MNs from hiPSCs, we used a previously reported protocol [25].

### Mice, treatment and behaviour analysis

SMA mouse models were previously described [15, 26, 27].

NMDA (Sigma-Aldrich) treatment was performed as described [15] and AA147 (Sigma-Aldrich) was injected intrathecally into P7 neonatal control and severe SMA-like mice. Grip strength and the ambulatory behaviour were assessed as described [15].

The care and treatment of animals followed the national authority's (French Ministry of Research and Technology) guidelines for the detention, use and ethical treatment of laboratory animals.

### Western blot analysis

Western blots were performed as described previously [28, 29]. Antibodies are detailed in the Supporting Information.

### RT-qPCR analysis

RT-qPCR was performed as described [30]. Relative mRNA amounts were quantified using the  $2^{-\Delta\Delta CT}$  method [31].

### Immunofluorescence analysis

Immunofluorescence on hiPSCs and motor neuron was performed as described previously [15, 25, 29].

### Cell culture and plasmid transfection

Human immortalised cultures of fibroblasts from type I SMA patients [32] were transfected with a plasmid coding for XBP1s fused to a flag (pCMV5-Flag-XBP1s). pCMV5-Flag-XBP1s was a gift from Qingbo Xu and Lingfang Zeng (Addgene plasmid # 63680; <http://n2t.net/addgene:63680>; RRID:Addgene\_63680) [33]. SMA and WT human primary cultures of myoblasts were cultivated as described previously [30, 34]. MN-1 [35] cells were transfected with siRNA (Dharmacon) following the manufacturer's instructions.

## Chromatin immunoprecipitation (ChIP)

SMA fibroblasts were transfected for 48 h with pFlag-CMV2-empty vector or pCMV5-Flag-XBP1s. Chromatin was extracted and DNA was fragmented. After Flag immunoprecipitation, bound DNAs were analysed by qPCR.

## Statistical analysis

All data are expressed as means with standard deviation ( $\pm$  SD) of  $n$  different cultured cell samples or mice for each group. Grubbs' test was performed to remove potential outliers.

For endpoint studies, a Kolmogorov–Smirnov normal distribution analysis was performed followed by the appropriate statistical test indicated in the figure legends (Prism 7, GraphPad Software, Inc).

## Experimental design

All experiments based on mice were performed blinded, with sample vials uniquely coded to replace pathological or control origins. The pathological background of the mice was further determined by both physiological criteria (body weight, size and tail length) and post-dissection genotyping.

## RESULTS

### XBP1s expression is impaired in hiPSC-derived motor neurons of severe type SMA patients

Previous studies reported either enhanced [23] or unchanged [24] levels of XBP1s mRNA in MNs derived from hiPSCs of SMA patients. To clarify the status of the IRE1 $\alpha$ /XBP1 pathway in SMA MNs, we generated hiPSC-derived MNs from two different type I SMA patients (cell lines 232C11 and 13C2) and two controls (cell lines 56C2 and 14C5) [25]. Among the hiPSC samples, we used one SMA (13C2) and one control (14C5) that displayed a direct familial link (mother and child) (Figure S1A). The other cell lines were totally independent. To attribute potential gene expression variation to changes in SMN expression change, a plasmid expressing SMN was stably transfected in the 13C2 SMA hiPSC line (Rescue). Moreover, we investigated the IRE1 $\alpha$ /XBP1 pathway at two time points of MN differentiation, days 14 and 24, which correspond to new-born and mature MNs, respectively [25]. SMN expression was significantly decreased in SMA hiPSC-derived MNs compared with controls, but over-expressed in the rescue (Figure S1B).

To assess the purity of MN in our cultures, we evaluated the percentage of MNs in control, SMA and Rescue hiPSC-derived cultures using HB9 and ISL1 co-immunostaining (Figure S1C). As reported [25], we obtained 70% HB9 positive cells, that is, MNs, in all cultures at day 14 (Figure S1D,E). We next evaluated MN survival from day

14 to day 24, by counting ISL1 positive cells. While no cell death could be detected at day 14 in any of the conditions, we observed an increase of about 40% cell death at day 24 in SMA hiPSC-derived MNs compared with controls (Figure S1F). As expected, the level of cell death in Rescue hiPSC was significantly lower than in SMA hiPSC and comparable to controls (Figure S1F).

We first analysed the mRNA levels of the main effectors of IRE1 $\alpha$ /XBP1 pathway, namely, *IRE1 $\alpha$* , *XBP1u* and *XBP1s*, and the XBP1s-target *Bip/GRP78* (Figures 2A,C and S2). We unexpectedly found a decrease in *XBP1s* expression in SMA hiPSC-derived MNs compared with controls. This decrease was significant at day 14 but not at 24. Importantly, *XBP1s* mRNA expression reached levels comparable to controls in the rescue condition. No difference in *XBP1u*, *IRE1 $\alpha$*  and *Bip/GRP78* expression was witnessed irrespective of the time of differentiation (Figures 2A,C and S2). Moreover, *XBP1s* mRNA expression was significantly decreased in the 13C2 SMA MNs at day 14 compared with the family linked 14C5 control MNs (Figures 2E and S1).

Since these data suggested an inhibition of the IRE1 $\alpha$ /XBP1 pathway in SMA MNs, contrary to what has been previously reported [23], we analysed the protein expression of IRE1 $\alpha$  and XBP1s in SMA MNs. Importantly, and consistent with the mRNA results, XBP1s protein level at day 14 was decreased more than 50% compared with control hiPSC (Figure 2B). We then assessed the activation of IRE1 $\alpha$  in SMA MNs at day 14, and found no difference in phosphorylated IRE1 $\alpha$  or total IRE $\alpha$  expression levels. This disconnection between XBP1s expression and IRE1 $\alpha$  activation pattern occurred in both the immature and mature MNs (Figure S1F). Despite significant over-activation of IRE1 $\alpha$  in SMA at 24 day, XBP1s expression is unchanged in SMA MNs compared with controls (Figure 2D). Thus, during SMA MN differentiation, XBP1s depletion unexpectedly precedes IRE1 $\alpha$  activation and, thereafter (d24), overactivated IRE1 $\alpha$  failed in producing large amounts of XBP1s compared with controls.

Because XBP1s depletion in SMA MNs might activate pro-apoptotic pathways, we analysed the expression of *CHOP*, a marker of the shift from pro-survival to pro-apoptotic UPR. As shown in Figure S2, and in contrast to previously reported data [23], no alteration of *CHOP* expression was found in SMA hiPSC-derived MNs compared with controls.

These data indicate that the IRE1 $\alpha$ /XBP1 pathway is compromised in SMA MNs, with an unexpected SMA-induced decrease in XBP1s expression which likely precedes MN cell death.

### The IRE1 $\alpha$ /XBP1 branch of the UPR is compromised in non-neuronal SMA patient cells

SMA is not restricted to MNs and many tissues are affected by SMN depletion [36] including skeletal muscle, which has been found to be a critical contributor to SMA pathophysiology [37]. Thus, we investigated the status of the IRE1 $\alpha$ /XBP1 pathway in several human SMA samples, including muscle cells. We studied the IRE1 $\alpha$ /XBP1 pathway in a primary culture of myotubes derived from a severe type SMA

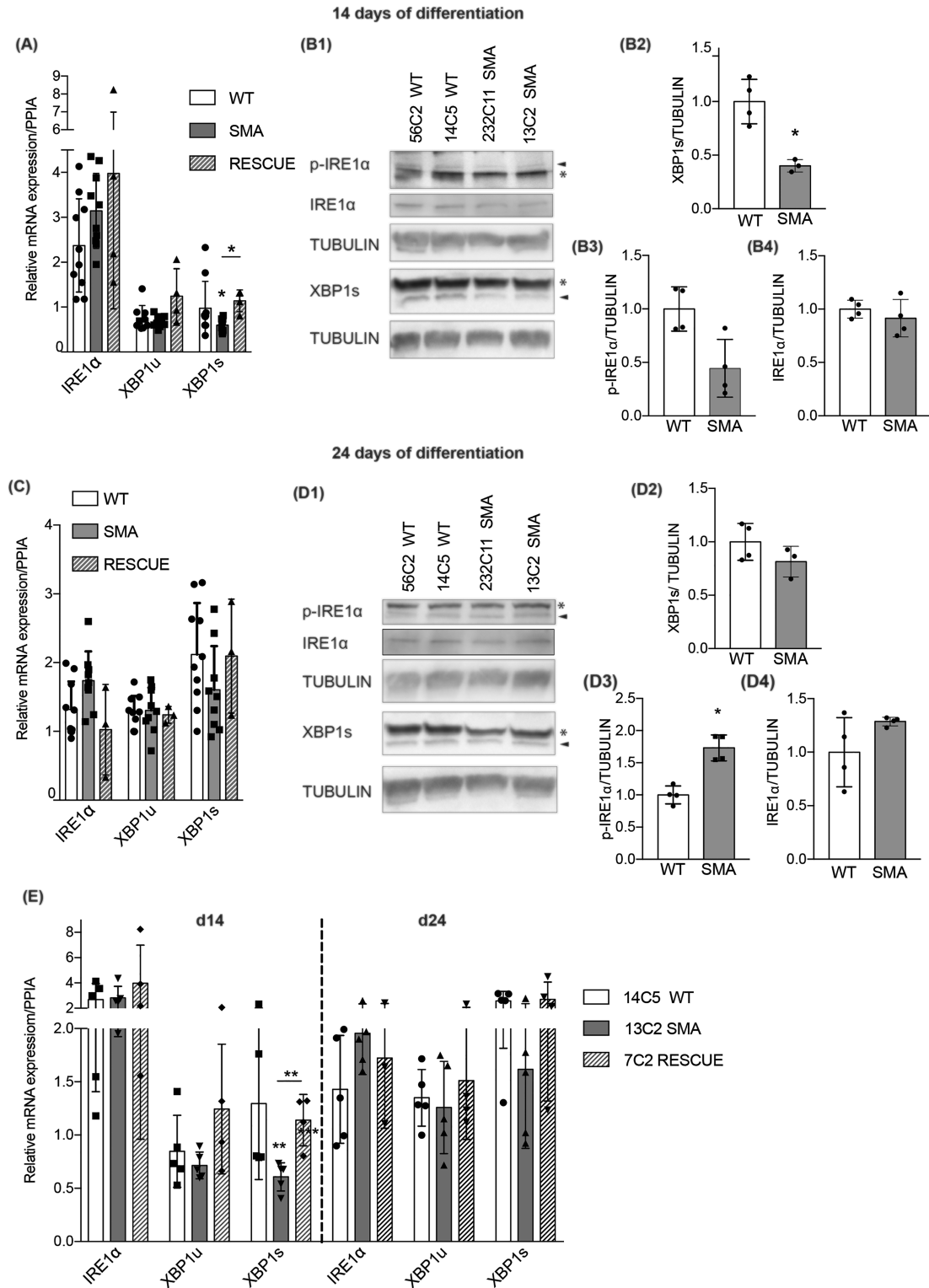


**FIGURE 2** Differentiated MNs from SMA hiPSCs show a defect in XBP1 splicing. (A, C) Quantification by RT-qPCR of *IRE1α*, *XBP1u* and *XBP1s*, mRNAs normalised to *PP1A* transcript in differentiated MNs, at day 14 (d14) (A) and day 24 (d24) (C) from WT, SMA and rescue cell line hiPSCs ( $n = 2$  WT and SMA and  $n = 5$  technical replicates). (B, D) Quantification by western blot of p-IRE  $\alpha$  *IRE1α* and *XBP1s*, in differentiated MNs, at d14 (B) and d24 (D) ( $n = 2$  WT and SMA and  $n = 3$  technical replicates). (E) Quantification by RT-qPCR of *IRE1α*, *XBP1u* and *XBP1s* mRNAs normalised to *PP1A* transcript at d14 and d24 from the control 14C5 and the SMA 13C2 (mother and child, respectively) and the rescue cell line hiPSCs. Data are expressed as mean  $\pm$  SD, \* $p < 0.05$ , non-parametric Mann-Whitney  $U$  test

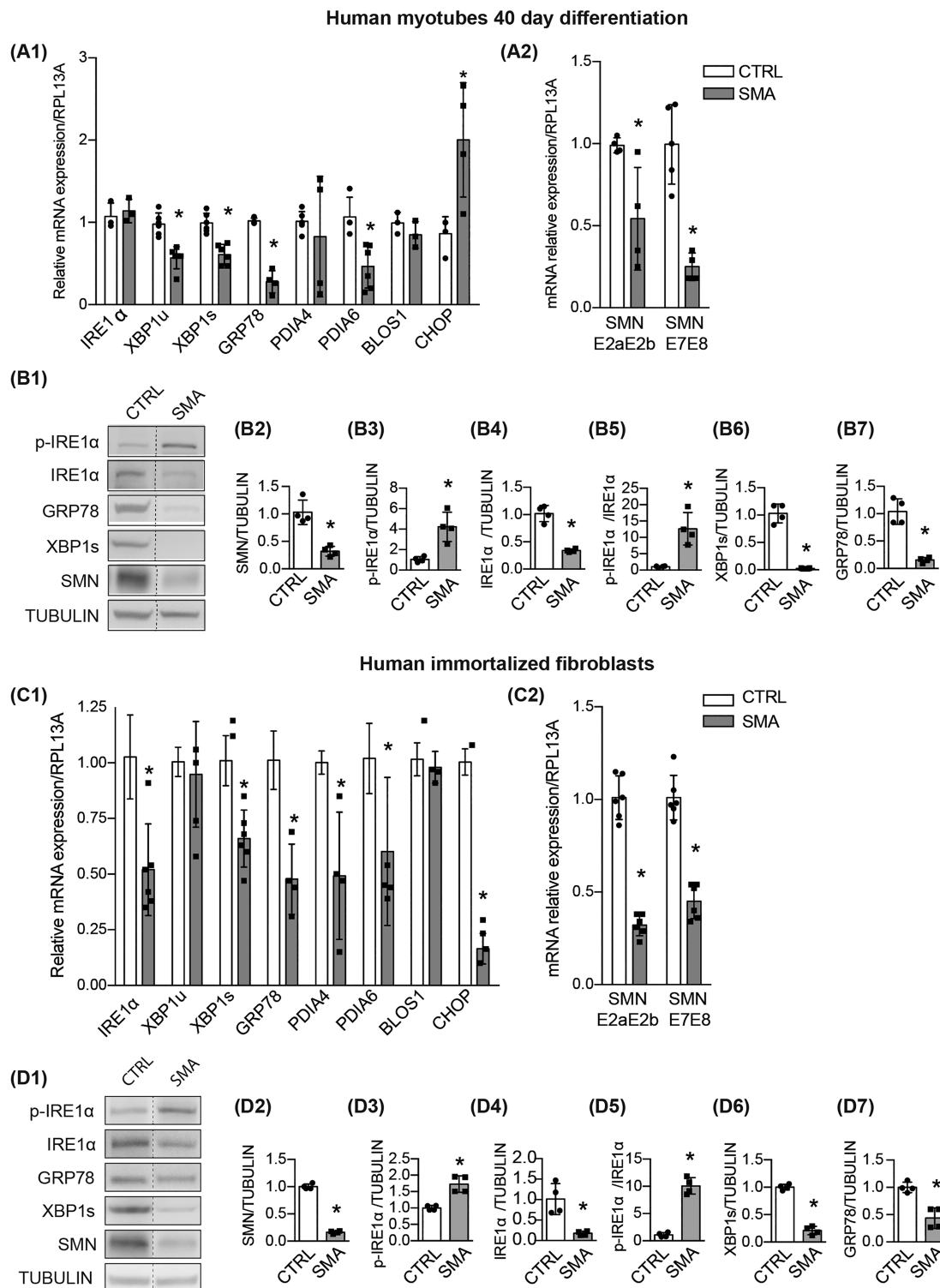


**FIGURE 3** IRE1 $\alpha$ /XBP1 pathway is altered in human SMA patient-derived myotubes and fibroblasts. (A) Quantification by RT-qPCR of IRE1 $\alpha$ , XBP1u, XBP1s, BiP/GRP78, PDIA4, PDIA6, BLOS1, CHOP (A1) total SMN exon-2a–exon-2b (SMNE2aE2b) and SMN-containing exon 7, exon-7–exon-8 (SMNE7E8) mRNAs (A2) normalised to RPL13A transcript in SMA type II patient-derived myotubes after 40 days of differentiation ( $n = 4$ ). (B) Western blot analysis and quantification of p-IRE1 $\alpha$ , IRE1 $\alpha$ , XBP1s, SMN and BiP/GRP78 protein expression in SMA type II patient-derived myotubes after 40 days of differentiation ( $n = 4$ ). (C) Quantification by RT-qPCR of IRE1 $\alpha$ , XBP1u, XBP1s, BiP/GRP78, PDIA4, PDIA6, BLOS1, CHOP (C1) and SMNE2aE2b, SMNE7E8 mRNAs (C2) normalised to RPL13A transcript in SMA type I patient-derived immortalised fibroblasts ( $n = 4$ ). (D) Western blot analysis and quantification of p-IRE1 $\alpha$ , IRE1 $\alpha$ , XBP1s, SMN and BiP/GRP78 proteins expression in SMA type I patient-derived immortalised fibroblasts ( $n = 4$ ). Vertical dotted lines indicate that the pictures have been spliced from the same blot. Data are expressed as mean  $\pm$  SD \* $p < 0.05$  non-parametric Mann–Whitney  $U$  test

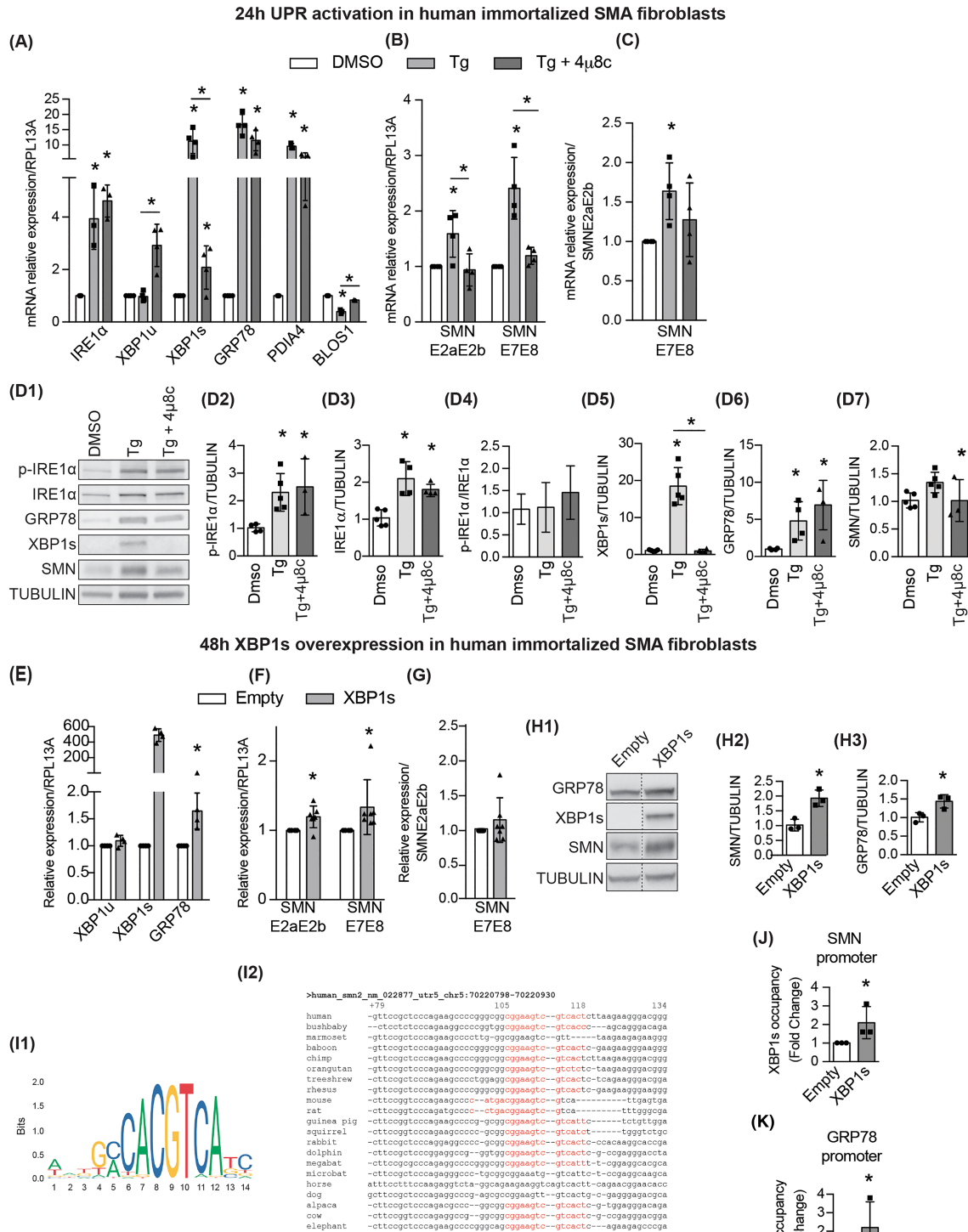


**FIGURE 4** Legend on next page.

**FIGURE 4** UPR stimulation increases SMN expression levels through the activation of IRE1 $\alpha$ /XBP1 pathway. (A, B) quantification by RT-qPCR of IRE1 $\alpha$ , XBP1u, XBP1s, BiP/GRP78, PDIA4 and BLOS1 (A) and SMNE2aE2b and SMNE7E8 mRNAs (B) normalised to RPL13A transcript ( $n = 4$ ) in SMA type I patient-derived immortalised fibroblasts treated with DMSO or 0.5  $\mu$ M thapsigargin (Tg-UPR inducer) with or without 4 $\mu$ 8c (IRE1 $\alpha$  RNase activity inhibitor) for 24 h. (C) Level of exon-7 inclusion in SMN transcript quantified by RT-qPCR of SMNE7E8 mRNAs normalised to SMNE2aE2b ( $n = 4$ ) in SMA type I patient-derived immortalised fibroblasts treated with DMSO or 0.5  $\mu$ M Tg with or without 4 $\mu$ 8c for 24 h. (D) Western blot analysis and quantification of p-IRE1 $\alpha$ , IRE1 $\alpha$ , XBP1s, BiP/GRP78 and SMN proteins ( $n = 4$ ) in SMA type I patient-derived immortalised fibroblasts treated with DMSO or 0.5  $\mu$ M Tg with or without 4 $\mu$ 8c for 24 h. \* $p < 0.05$ . One-way ANOVA post hoc Tukey test. (E, F) Quantification by RT-qPCR of XBP1u, XBP1s, BiP/GRP78 (E) and SMNE2aE2b or SMNE7E8 (F) mRNAs normalised to RPL13A transcript in SMA type I patient-derived immortalised fibroblasts transfected 48 h with pCMV5-flag-XBP1s or empty vector pFlag-CMV2 ( $n = 6$ ). (G) Quantification by RT-qPCR of SMNE7E8 mRNAs normalised to SMNE2aE2b ( $n = 6$ ) in SMA type I patient-derived immortalised fibroblasts transfected 48 h with pCMV5-flag-XBP1s or empty vector pFlag-CMV2. (H) Western blot analysis and quantification of SMN and BiP/GRP78 protein expression in SMA type I patient-derived immortalised fibroblasts transfected 48 h with pCMV5-flag-XBP1s 0.5  $\mu$ g or the empty vector (pFlag-CMV2-empty) ( $n = 3$ ). \* $p < 0.05$ . Non-parametric Mann–Whitney  $U$  test. (I) A XBP1 binding site is present in SMN gene. CORE sequence of the consensus XBP1s binding from JASPAR database [39] (XBP1 JASPAR\_CORE\_2016, MA0844.1, MA0844.1) (I1). Alignment of the 5'UTR of human SMN2 gene contains a XBP1s binding site conserved among mammals (analyse done on ConTrav3 web site [40]) (I2). XBP1s binding site labelled in red is located in the first exon of SMN2 gene. (J, K) qPCR performed to detect SMN2 (J) and BiP/GRP78 (K) promoters following ChIP against flag-XBP1s in SMA type I patient-derived immortalised fibroblasts transfected 48 h with 0.5  $\mu$ g of pCMV5-flag-XBP1s or the empty pFlag-CMV2 vectors ( $n = 3$ ). Data are expressed as mean  $\pm$  SD \* $p < 0.05$ . Non-parametric Mann–Whitney  $U$  test. Vertical dotted lines indicate that the pictures have been spliced from the same blot

patient, after 40 days of differentiation [34]. We first analysed the expression levels of the main effectors of the pathway at the RNA level. We found that *XBP1u*, *XBP1s*, *BiP/GRP78* and *PDIA6* mRNAs were significantly downregulated in SMA myotubes compared with controls, whereas *IRE1 $\alpha$*  and *PDIA4* mRNA levels remained unchanged (Figure 3A).

At the protein level, total IRE1 $\alpha$  expression was significantly decreased along with a 10-fold increase in IRE1 $\alpha$  phosphorylation in SMA myotubes compared with controls (Figure 3B). This overactivation of IRE1 $\alpha$  is disconnected from XBP1s production, since XBP1s protein reached almost undetectable levels in SMA myotubes, and the XBP1s-target BiP/GRP78 protein was dramatically reduced (Figure 3B).

We next investigated whether XBP1s depletion in SMA myotubes could induce pro-apoptotic pathways. We first analysed the expression levels of *CHOP* mRNA and found a significant increase of this pro-apoptotic marker in SMA myotubes compared with controls (Figure 3A). We next analysed the expression of *BLOS1*, considered a universal target of RIDD, which promotes apoptosis through IRE1 $\alpha$  nuclease activity [38]. No alteration of *BLOS1* mRNA levels was found in SMA myotubes compared with controls (Figure 3A).

We repeated this analysis in cultures of SMA patient fibroblasts, which constitute a convenient cell model to analyse molecular defects dependant on SMN depletion [32]. The SMA fibroblasts globally reproduced the picture of IRE1 $\alpha$ /XBP1 pathway impairments we had found in SMA myotubes, except for *CHOP* expression (Figure 3C,D). Again, we found that a 10-fold IRE1 $\alpha$  overactivation was associated with a significant decrease in XBP1s and its target BiP/GRP78 expression levels (Figure 3D).

These results confirm a dysfunction of the IRE1 $\alpha$ /XBP1 branch of the UPR in SMA with low expression of one main effector component of the pathway, namely XBP1s, despite overactivation of the pathway initiator IRE1 $\alpha$ .

### The activation of the IRE1 $\alpha$ /XBP1 pathway increases SMN expression levels in SMA fibroblasts

We next wondered whether XBP1s increase via UPR activation in SMA cells could be beneficial, notably through SMN gene expression modulation. We treated SMA fibroblasts with Thapsigargin (Tg), a general activator of the three UPR branches and analysed IRE1 $\alpha$ /XBP1 components and SMN expression. Following Tg treatment, *IRE1 $\alpha$* , *XBP1s*, *BiP/GRP78* and *PDIA4* mRNA levels were significantly increased in comparison to DMSO-treated SMA fibroblasts (Figure 4A). As expected for the unspliced form of *XBP1*, *XBP1u* mRNA expression remained unchanged after Tg treatment. *BLOS1* mRNA was significantly decreased, as expected for a RIDD target.

To investigate the effects of Tg on SMN expression, we quantified the fraction of exon-7-containing mRNA inside the population of SMN transcripts using RT-qPCR aimed at either amplifying the exon-7–exon-8 segment (E7–E8) or the constitutive exon-2a–exon-2b segment (E2a–E2b) (Figure 4B,C). After Tg treatment in SMA fibroblasts, SMN mRNA expression was significantly enhanced, with a greater increase for exon-7-containing transcripts compared with the constitutive-exon transcripts, suggesting an exon-7 inclusion effect. All these data were confirmed at the protein level, notably the significant increase in XBP1s and SMN expression following UPR induction (Figure 4D).

To evaluate the contribution of the IRE1 $\alpha$ /XBP1 pathway to the increase in SMN expression among the three UPR branches, we inhibited IRE1 $\alpha$  RNase activity with 4 $\mu$ 8c [41] in Tg-treated SMA fibroblasts. In these conditions and as anticipated, *XBP1s* mRNA expression decreased and *XBP1u* mRNA accumulated, with no change in the expression of *IRE1 $\alpha$*  compared with DMSO-treated fibroblasts (Figure 4A). *BiP/GRP78* expression remained stable, as expected for a target of the three UPR branches. Moreover, *BLOS1* mRNA reached expression levels comparable to DMSO-treated fibroblasts,

confirming the efficiency of the 4 $\mu$ 8c treatment as an IRE1 $\alpha$  RNase inhibitor. Importantly, *SMN* mRNA expression enhancement following UPR induction in SMA fibroblasts was abolished by IRE1 $\alpha$  inhibition, including full-length and  $\Delta$ 7 *SMN* transcripts (Figure 4B,C). All these data were confirmed at the protein level, with the return of XBP1s and SMN expression to pathological levels after IRE1 $\alpha$  RNase inhibition (Figure 4D). Since 4 $\mu$ 8c inhibits the RNase catalytic domain of IRE1 $\alpha$  without interfering with its kinase activity, no difference was recorded in IRE1 $\alpha$  phosphorylation after 4 $\mu$ 8c treatment [41].

Thus, reactivating the IRE1 $\alpha$ /XBP1 branch of UPR in SMA cells induces an upregulation of SMN expression that is specifically dependent on IRE1 $\alpha$  RNase activity.

### XBP1s is a transcriptional regulator of *SMN2* gene

To investigate whether *SMN* expression could be regulated by XBP1s, we transfected SMA fibroblasts with a plasmid encoding XBP1s fused with a Flag tag [33]. XBP1s overexpression significantly enhances *SMN* expression both at the mRNA (Figure 4F,G) and at the protein level (Figure 4H). Additionally, RT-qPCR experiments revealed the same increase of both *SMN* full-length and  $\Delta$ 7 *SMN* transcripts, suggesting therefore that XBP1s promoted steady state levels of *SMN* transcripts and not exon-7 splicing (Figure 4F,G). Moreover, XBP1s overexpression in SMA fibroblasts significantly increased BiP/GRP78 expression, as expected for a XBP1s gene target.

XBP1s is a transcription factor that preferentially binds CRE-like sequences containing an ACGT core in target gene promoters [42, 43]. We previously reported a CRE sequence in the human *SMN* promoter (GenBank accession AF187725), in the first exon of *SMN* (+105 to +118 base pairs) [30]. This site, which can be also bound by the CREB protein, is considered as a crucial positive regulator of *SMN* gene expression [30]. Therefore, we performed an in silico analysis to determine if XBP1s could bind the *SMN2* promoter and particularly on this CRE site [40]. As shown in Figure 4I, the CRE site is also a consensus XBP1s binding site that is highly conserved in mammals. Therefore, we investigated whether XBP1s could bind this site by performing ChIP experiments in SMA fibroblasts overexpressing Flag-XBP1s using Flag antibody. We found that XBP1s binds to the *SMN* promoter, as well as the *BiP/GRP78* promoter used as a positive control (Figure 4J,K).

These data highlight an unanticipated role of XBP1s in directly activating *SMN2* gene expression in SMA cells and strongly suggest that enhancing XBP1s expression could be beneficial for SMA.

### The IRE1 $\alpha$ /XBP1 branch of the UPR is compromised in the spinal cord of severe SMA-like mice

These results prompted us to investigate the activation status of the IRE1 $\alpha$ /XBP1 pathway in the spinal cord of control and severe SMA-like mice, with or without NMDA-receptor activation, since this treatment also increases SMN expression [15] and activates the UPR [16].

We first analysed the expression levels of the main effectors of the pathway, at the mRNA and the protein level in the lumbar spinal cord of severe SMA-like mice at P12, which corresponds to end-stage disease in this mouse model. As shown in Figure 5A, we found that *Ire1 $\alpha$*  mRNA was overexpressed in SMA spinal cord compared with controls, whereas *Xbp1u* and *Xbp1s* mRNAs were significantly down-regulated. Moreover, we found a strong increase in phosphorylated IRE1 $\alpha$  (p-IRE1 $\alpha$ ), without an increase in total IRE1 $\alpha$  protein (Figure 5B). The significant increase in the p-IRE1 $\alpha$ /IRE1 $\alpha$  ratio in SMA compared with controls, strongly suggests that IRE1 $\alpha$  was over-activated in SMA, as previously reported in another SMA mouse model [23]. As evidenced in human SMA cells, despite IRE1 $\alpha$  over-activation, XBP1s protein levels were significantly decreased (Figure 5B) along with the BiP/GRP78 protein. This result concurred with the decrease in the mRNA expression of XBP1s targets *BiP/Grp78*, *Pdia4* and *Pdia6* in SMA spinal cord compared with controls (Figure 5A).

Interestingly, NMDA-receptor activation rebalanced the expression of IRE1 $\alpha$ /XBP1 pathway components, including the up-regulation of XBP1s and BiP/GRP78 and the down-regulation of IRE1 $\alpha$ , leading to a pattern comparable to controls (Figure 5).

Again, *Chop* and *Blos1* expression levels remained unchanged in mouse SMA spinal cord with or without NMDA-receptor activation, suggesting an unlikely activation of IRE $\alpha$  dependent apoptotic pathways, including RIDD (Figure 5A).

These data suggest that in the spinal cord of severe SMA-like mice, as in SMA patient cells, IRE1 $\alpha$  although overactivated is unable to trigger pro-survival UPR cascade, and notably *Xbp1u* splicing, leading to XBP1s depletion.

### Alteration of the IRE1 $\alpha$ /XBP1 pathway precedes massive MN death in severe SMA-like mice

To determine whether the IRE1 $\alpha$ /XBP1 branch alteration, notably the depletion of XBP1s, precedes or is a consequence of SMA-induced MN death, we investigated protein expression levels and the activation status of IRE1 $\alpha$ /XBP1 pathway in the lumbar spinal cord of severe SMA-like mice aged 4 (P4) and 8 (P8) days corresponding to pre-symptomatic and early symptomatic stages of the disease respectively, before the massive death of spinal MNs [26, 44]. Very interestingly, at P4, XBP1s expression displayed a significant downregulation in SMA spinal cord compared with controls, in the absence of any other molecular alteration of the pathway (Figure 6A). Later on, at P8, XBP1s protein levels remained significantly decreased in SMA spinal cord compared with controls. Moreover, at this age, the other main components of the IRE1 $\alpha$ /XBP1 pathway, that is, BiP/GRP78, IRE1 $\alpha$  and p-IRE1 $\alpha$  proteins displayed a significant decrease in their protein expression (Figure 6B). Interestingly, the ratio of p-IRE1 $\alpha$ /total IRE1 $\alpha$ , remained unchanged when compared with controls, suggesting that defects in the IRE1 $\alpha$ /XBP1 pathway precede IRE1 $\alpha$  overactivation in SMA spinal cord as previously seen in SMA hiPSC. In addition, we investigated whether the IRE1 $\alpha$ -XBP1 pathway was the only branch

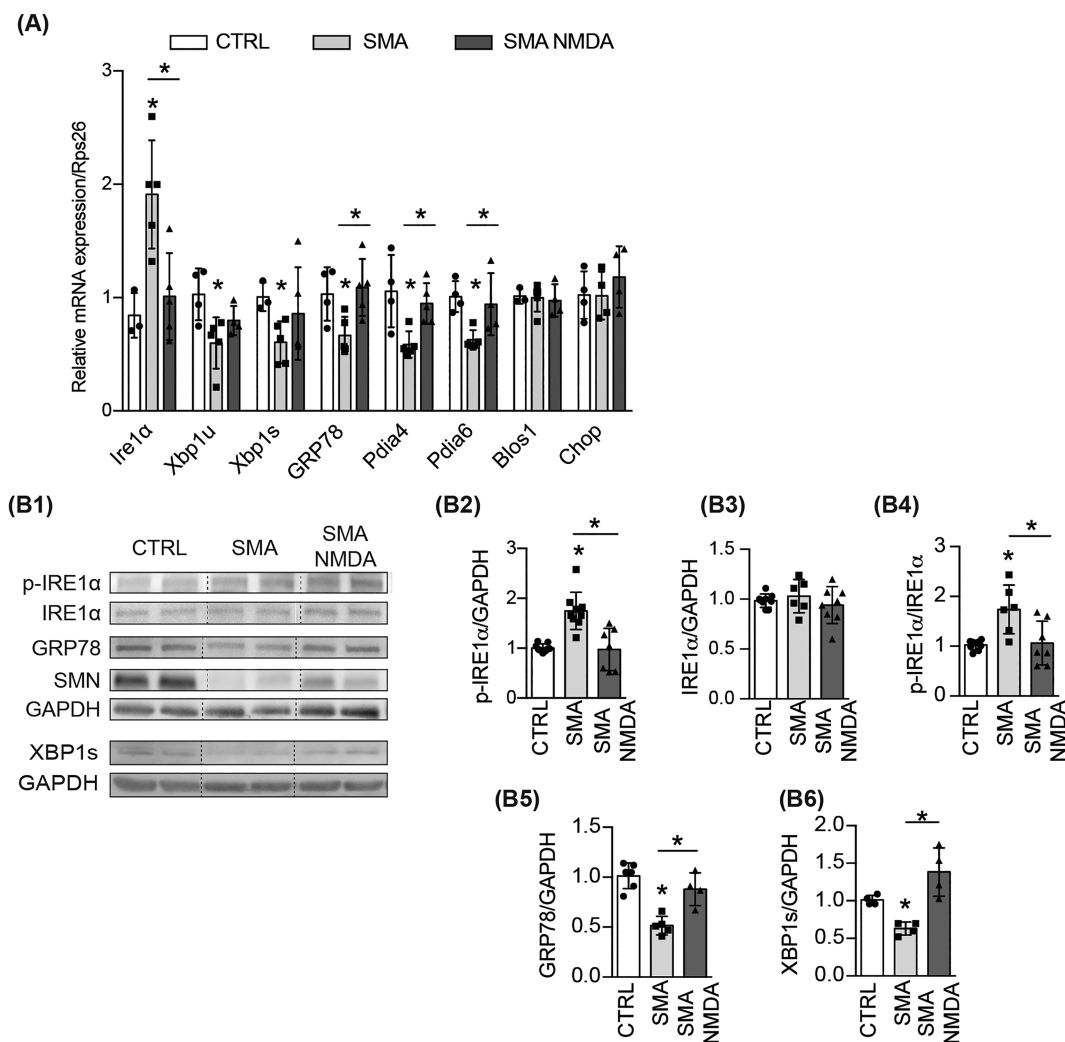


**FIGURE 5** The IRE1 $\alpha$ /XBP1 branch of the UPR is compromised in the spinal cord of severe SMA-like mice. (A) Quantification by RT-qPCR of *Ire1 $\alpha$* , *Xbp1u*, *Xbp1s*, *Bip/Grp78*, *Pdia4* and *6*, *Blos1* and *Chop* mRNAs normalised to *Rps26* in the spinal cord of vehicle-treated control mice and vehicle- or NMDA-treated severe SMA-like mice at 12 days of age ( $n = 4$ ). (B) Western blot analysis and expression quantification of p-IRE1 $\alpha$ , IRE1 $\alpha$ , BiP/GRP78, SMN and XBP1s proteins in the spinal cord of vehicle-treated control mice and vehicle- or NMDA treated severe SMA-like mice at 12 days of age ( $n = 6$ ). Data are expressed as mean  $\pm$  SD \* $p < 0.05$ . One-way ANOVA post hoc Tukey test. Vertical dotted lines indicate that the pictures have been spliced from the same blot

of the UPR altered in the lumbar spinal cord of SMA-like mice. We did not find any alteration of ATF6, PERK or ATF4 at the mRNA level at P8 and P10 compared with controls (Figure S3A,B). Nevertheless, we found by western blot that ATF4 and the activated form of ATF6 (cleaved ATF6) were decreased at P10 in the spinal cord of SMA-like mice compared with controls (Figure S3C). Thus, the activation of the three UPR effectors is impaired in the spinal cord of SMA-like mice at late stages of the disease.

We extended our analysis to the lumbar spinal cord of other mouse models of SMA, including very severe SMA-like mice [27], in which massive MN death occurs at birth, and the mild-type SMA-like mice [45], in which MN death is milder and progressive compared with the former. Interestingly, the same expression defects in IRE1 $\alpha$ /XBP1 pathway as those found in severe SMA-like mice aged of 12 days could be observed in the spinal cord of very severe SMA-like mice at 2 days of age, including *Xbp1s* and *Bip/Grp78* expression

downregulation and IRE1 $\alpha$  overexpression (Figure S3D). By contrast, no alteration in the IRE1 $\alpha$ /XBP1 pathway could be found in the spinal cord of mild-type SMA-like mice (Figure S3E).

These data show that IRE1 $\alpha$ /XBP1 pathway alteration, notably the decrease in XBP1s expression, is associated with, and even precedes, MN death in severe types of SMA-like mice, suggesting that IRE1 $\alpha$ /XBP1 alterations participate in SMA pathogenesis.

### In vitro SMN depletion in murine MN-like cells recapitulates the IRE1 $\alpha$ /XBP1s alterations found in vivo

We next investigated whether IRE1 $\alpha$ /XBP1s impairments found in SMA could be a direct consequence of SMN depletion. We used the murine Motor-Neuron-1-like (MN-1) cell line and depleted SMN by

about 75%. This induced significant IRE1 $\alpha$  overactivation (Figure 6C) associated with a significant decrease in XBP1s expression, at the mRNA and protein levels (Figure S4; and Figure 6C). The decrease of XBP1s expression was associated with a concomitant decrease in its target BiP/GRP78, but only at the protein level.

Thus, SMN depletion in MN-1 cells was sufficient to compromise the IRE1 $\alpha$ /XBP1 pathway, with, notably, an induced XBP1s depletion and IRE1 $\alpha$  overactivation.

### Enhancement of XBP1s levels by pharmacologic ATF6-activating molecule promoted SMN expression

Since XBP1s could induce SMN expression and since IRE $\alpha$  is overactivated in SMA cells, we hypothesise that increasing XBP1u

expression should provide enough substrates to IRE1 $\alpha$  to restore XBP1s expression. Therefore, knowing ATF6 activates XBP1 transcription [20], we used a specific ATF6 activator called AA147 shown to promote protective remodelling of UPR system [46]. AA147 treatment in SMA fibroblasts was sufficient to significantly increase XBP1u mRNAs levels (Figure 7A) and as anticipated, XBP1s. The mRNA expression of XBP1s gene targets BiP/GRP78 and CHOP was also increased. We found that only the exon-7 containing SMN transcripts displayed a significant enhancement following AA147 treatment, without change in the total amount of SMN transcripts (Figure 7B,C).

Therefore, we investigated AA147 treatment effects in vivo, in the spinal cord of severe SMA-like mice. These mice were treated daily from P7 to P10 by intrathecal injection of AA147. As expected, this treatment increased *Xbp1u* mRNA expression in the spinal cord of

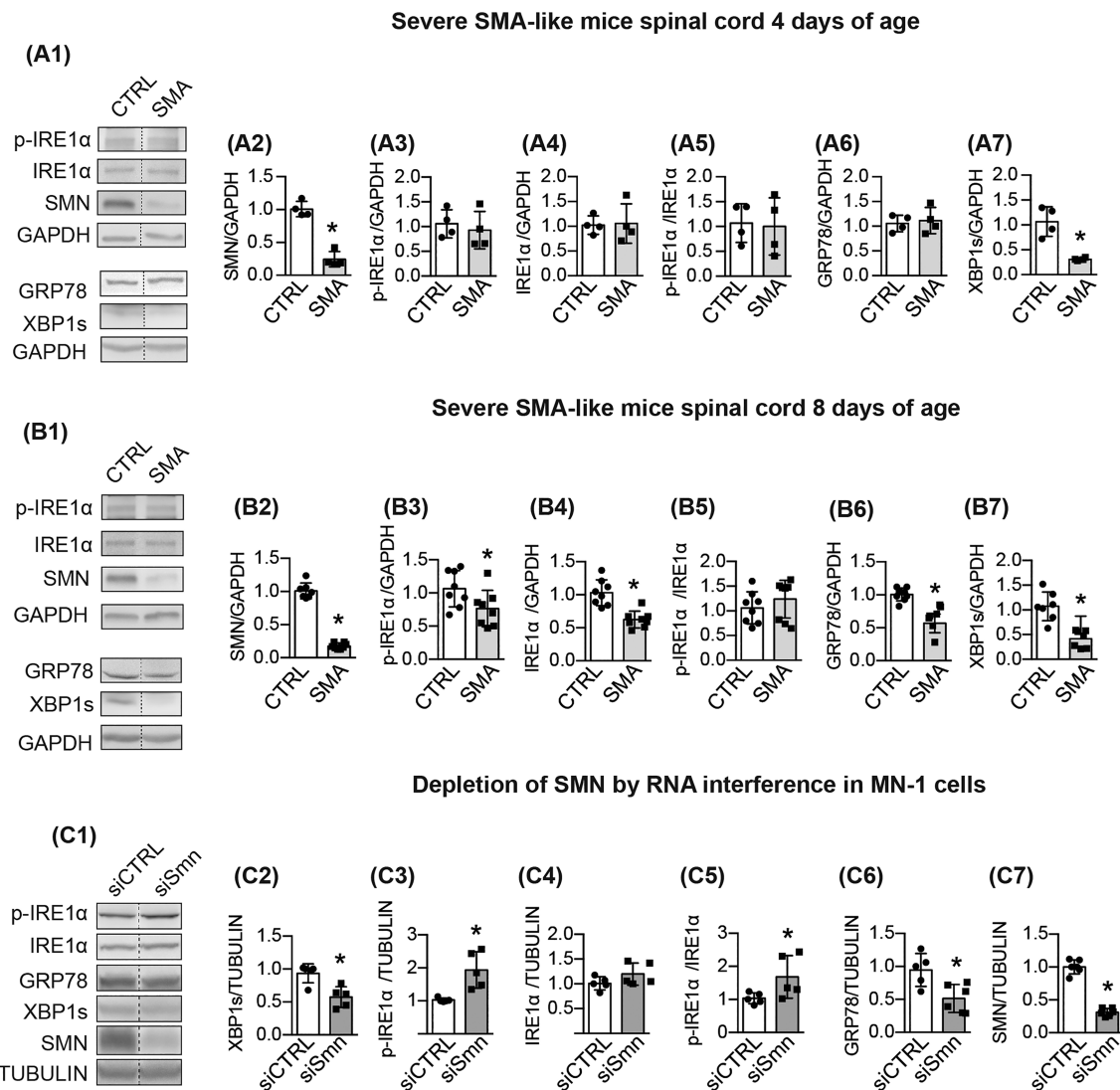


**FIGURE 6** XBP1s diminution is an early event in severe SMA-like mice and is linked to SMN depletion. (A, B) Western blot analysis and quantification of SMN, p-IRE1 $\alpha$ , IRE1 $\alpha$ , XBP1s, BiP/GRP78 protein expression in the lumbar spinal cord of control and severe SMA-like mice at 4 days of age ( $n = 4$ ) (A) at 8 days of age ( $n = 4$ ) (B). (C) Western blot analysis and expression quantification of SMN, p-IRE1 $\alpha$ , IRE1 $\alpha$ , XBP1s and BiP/GRP78 proteins in MN-1 cell culture transiently transfected for 48 h with either a non-relevant siRNA (siCTRL) or a siRNA against murine *Smn* (siSmn) ( $n = 6$ ). Data are expressed as mean  $\pm$  SD. \* $p < 0.05$ . Non-parametric Mann-Whitney  $U$  test. Vertical dotted lines indicate that the pictures have been spliced from the same blot

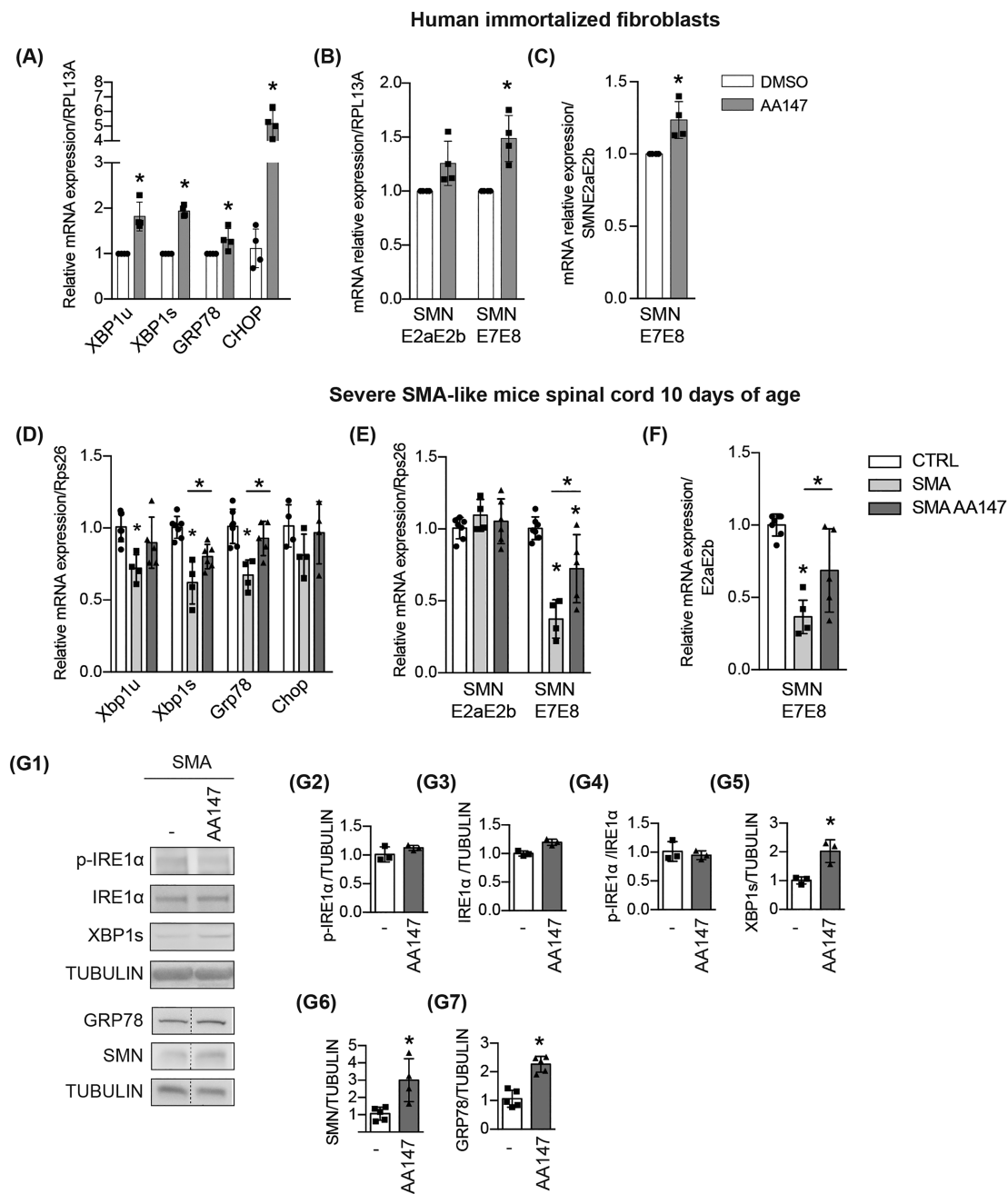


**FIGURE 7** ATF6-activating molecule AA147 enhances SMN expression in both in vitro and in vivo models of SMA. (A–C) SMA type I patient-derived immortalised fibroblasts were treated with DMSO or 20  $\mu$ M AA147 (ATF6 activator) ( $n = 4$ ) for 24 h. quantification by RT-qPCR of *XBP1u*, *XBP1s*, *Bip/GRP78* and *CHOP* (A) and *SMNE2aE2b* and *SMNE7E8* (B) mRNAs normalised to *RPL13A* transcript and of *SMNE7E8* mRNAs normalised to *SMNE2aE2b* (C). \* $p < 0.05$ . Non-parametric Mann–Whitney *U* test. (D–G) mRNA ( $n = 6$ ) (D–F) and protein ( $n = 5$ ) (G) expression analysis in lumbar spinal cord after injection of AA147 or vehicle in control and severe SMA-like mice from P7 to P10. Quantification by RT-qPCR of *Xbp1u*, *Xbp1s*, *Bip/Grp78* and *CHOP* (D) and *SMNE2aE2b* and *SMNE7E8* (E) normalised to *Rps26* transcript. Quantification by RT-qPCR of *SMNE7E8* mRNAs normalised to *SMNE2aE2b* (F). \* $p < 0.05$ . One-way ANOVA post hoc Tukey test. (G) Western blot analysis and quantification of p-IRE1 $\alpha$ , IRE1 $\alpha$ , XBP1 ( $n = 3$ ), SMN and BiP/GRP78 ( $n = 5$ ) protein expression. Data are expressed as mean  $\pm$  SD \* $p < 0.05$ . Non-parametric Mann–Whitney *U* test

severe SMA-like mice compared with vehicle-treated severe SMA-like mice, indicating ATF6 activation (Figure 7D). This activation was sufficient to re-activate the IRE1 $\alpha$ /XBP1 pathway since *Xbp1s* and *Bip/Grp78* mRNA levels were also increased. Interestingly, *Chop* mRNA was not increased after AA147 injection, suggesting that apoptosis

was not induced. Nevertheless, and consistent with the in vitro data, in vivo ATF6 activation resulted in a significant increase in exon-7 containing SMN transcripts (E7–E8), without increasing the amount of total SMN mRNA (E2a–E2b) (Figure 7E), showing that AA147 induced SMN exon-7 inclusion (Figure 7F). These results were confirmed at

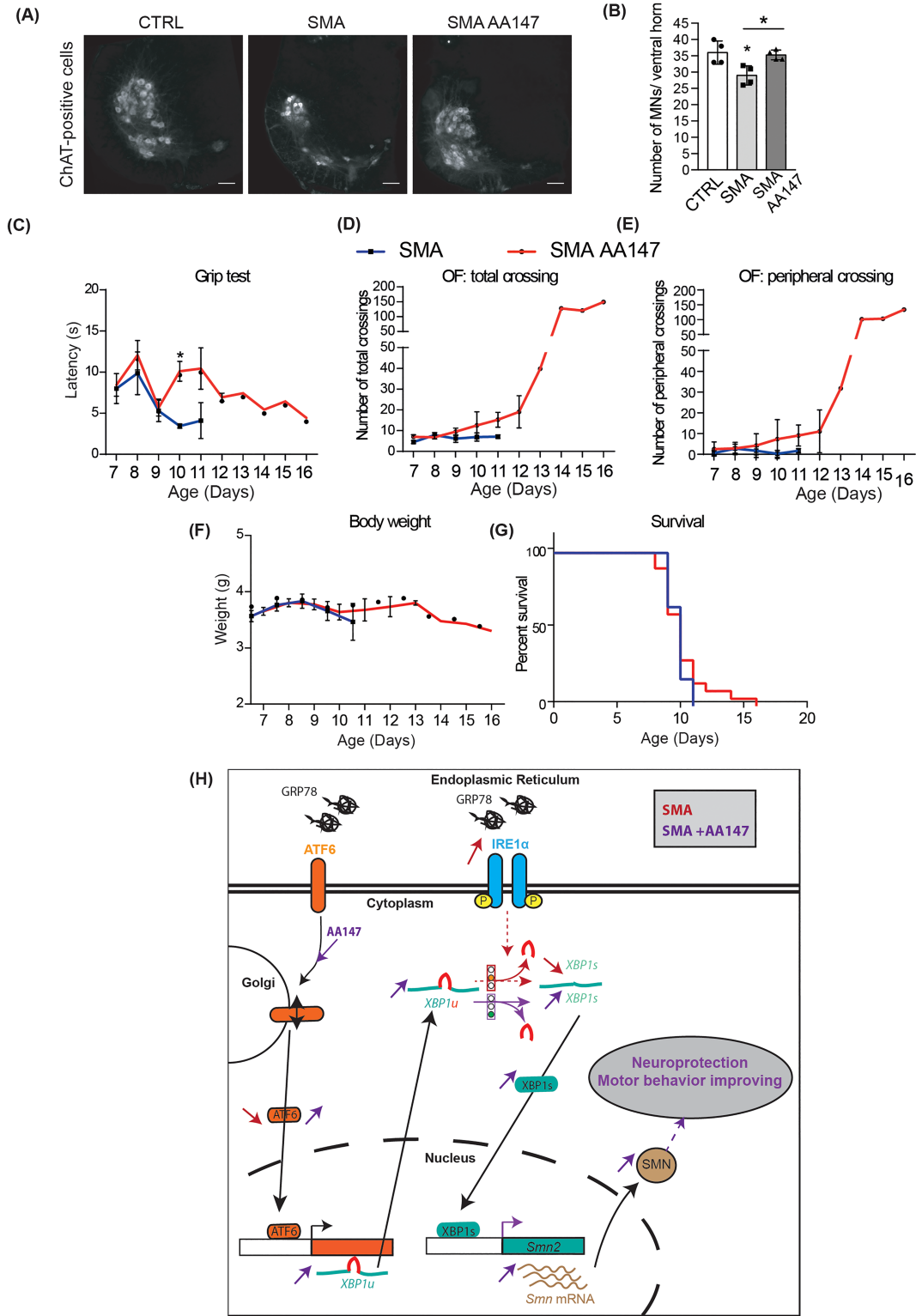


**FIGURE 8** Legend on next page.

**FIGURE 8** In vivo AA147 treatment in severe SMA-like mice promotes spinal MN protection and improves muscle function. (A) Immunodetection of ChAT-positive MNs in the lumbar spinal cord (L1–L5) of vehicle-treated control and SMA-like mice and AA147-treated severe SMA-like mice at 10 days of age and representative images are shown. Scale bar, 100  $\mu$ m. (B) Quantitative analysis of the number of MNs per ventral horn in the lumbar spinal cord of vehicle-treated control and SMA-like mice compared with AA147-treated severe SMA-like mice at 10 days of age ( $n = 4$ ).  $*p < 0.05$ . One-way ANOVA post hoc Tukey test. (C) Grip time, (D) total number of crossings during 5 min, (E) number of peripheral crossings of vehicle-, and AA147-treated severe SMA-like mice ( $n = 7$ ,  $n = 8$ , respectively).  $*p < 0.05$ . Non-parametric Mann–Whitney  $U$  test. (F) Weight curve and (G) lifespan in AA147-treated ( $n = 20$ ) compared with vehicle-treated severe SMA-like mice ( $n = 17$ ). Data are expressed as mean  $\pm$  SD. (H) Proposed molecular mechanisms of ATF6 activation in SMA leading to SMN expression increase, neuroprotection and motor behaviour improving. AA147 treatment activates ATF6 by cleavage and then induces the transcription of *XBP1u* mRNA, the substrate of IRE $\alpha$ . This increase compensates the ineffective splicing of XBP1s despite IRE $\alpha$  overactivation and enhances the XBP1s expression. Therefore, XBP1s translocates in the nucleus and activates directly *SMN2* gene. Heightening SMN expression leads therefore to MN protection and motor behaviour improving

the protein level, in the spinal cord of AA147-treated compared with vehicle-treated severe SMA-like mice (Figure 7G). These changes in gene expression occurred without alteration in IRE1 $\alpha$  expression and activation (Figure 7G).

Altogether, these results show that ATF6 activation, directly in mouse SMA spinal cord, can enhance SMN expression, raising important questions on the neuroprotective potential of ATF6 pathway in SMA.

### Pharmacologic ATF6 activation limits MN loss and improves the motor behaviour of severe SMA-like mice

To determine whether ATF6-dependent SMN up-regulation would be associated with SMA spinal MN protection, we compared the number of ChAT-positive MNs in the ventral spinal cord of control mice and vehicle- or AA147-treated severe SMA-like mice at P10 (Figure 8A,B). We observed 20% MN loss in the vehicle-treated severe SMA-like mice in comparison to controls. Interestingly, after AA147 treatment, the number of spinal MNs was no longer different from healthy controls. Thus, ATF6 activation exerted a neuroprotective effect on the MNs.

We next questioned whether this neuroprotection following AA147 treatment would improve the motor behaviour of severe SMA-like mice. We first subjected the mice to a grip test and found that AA147 treatment significantly increased the grip time of severe SMA-like mice at P10 (Figure 8C). We then analysed the spontaneous activity of the mice in an open field (Figure 8D,E). Compared with vehicle-treated severe SMA-like mice, severe SMA-like mice treated with AA147 showed a progressive and continuous increase in their exploratory activity, with a total number of crossings that doubles from P8 to P11, including more exploration at the edges of the field.

We next looked at the body weight curves of mice. While the severe SMA-like mice, as expected, displayed a severe body weight reduction from P8 until death that occurred around 10 days of age, the AA147-treated severe SMA-like mice maintained their weight until death (Figure 8F).

Finally, we found that 30% of AA147 treated mice survived longer than the 10 day's mean lifespan of the vehicle-treated severe SMA like-mice (Figure 8G).

Taken together, these data demonstrate that in vivo ATF6 activation significantly limited the extent of SMA-induced MN death, associated with the improvement of the motor behaviour of severe SMA-like mice.

## DISCUSSION

This study shows that the depletion of active XBP1, independent of the activation status of its inducer IRE1 $\alpha$ , participates in SMA-induced neurodegeneration. This effect likely occurs through the lack of XBP1s-mediated enhancement of SMN expression. XBP1s depletion, which likely precedes IRE1 $\alpha$  overactivation, can be rescued by ATF6 induction in vivo, leading to MN protection and significant improvements of SMA symptoms in mice (Figure 8H).

One key finding is that XBP1s depletion in SMA worsens the SMN defect. Indeed, *SMN* genes are transcriptional targets of XBP1s, as evidenced by both the enhancement in SMN expression following XBP1s overexpression in SMA cells and XBP1s ability to bind *SMN2* promoter (Figure 4). The role of XBP1s as a transcriptional activator of genes with unknown links to ER stress such as those involved in cell differentiation has already been reported [47, 48]. Interestingly, XBP1s may also contribute to the promotion of exon-7 inclusion in *SMN* transcripts generated by *SMN2* transcription, as observed following ATF6 activation by AA147 or global UPR activation by thapsigargin. However, this event was not observed when XBP1s alone was overexpressed, suggesting that other UPR branches, such as ATF6, are needed for regulating *SMN2* splicing. Interestingly, XBP1s and ATF6 have been already shown to act in synergy for controlling gene expression [49, 50].

In SMA, in which the accumulation of unfolded proteins has never been demonstrated, the SMA-induced XBP1s depletion is a likely explanation for IRE1 $\alpha$  overactivation. The earliest event of the pathway alteration found in SMA patient hiPSC-derived MNs was XBP1s expression decrease after 14 days of differentiation, thus before the massive MN death that begins at day 18 (Figure S1). In line with these

results, XBP1s decrease was the unique alteration of the pathway seen in the spinal cord of severe SMA-like mice at P4 (Figure 6). Alterations in IRE1 $\alpha$  activation could be detected in a later point during SMA progression. Thus, in all the severe SMA models we used, which include hiPCS-derived MNs, human myotubes and fibroblasts, SMN-depleted murine MN-like cells and two different severe type SMA-like mouse strains, XBP1s was depleted, irrespective of IRE1 $\alpha$  activation pattern. As reported previously, XBP1s depletion in pancreas  $\beta$ -cells is sufficient to cause constitutive overactivation of IRE1 $\alpha$  and impairments in ER stress response [51].

Why SMN deficiency can result in XBP1s depletion remains to be elucidated. Interestingly, XBP1s protein stability is under the control of AKT signalling pathway [52]. Because AKT is constitutively inhibited in SMA [15], it might induce XBP1s protein destabilisation. Concurring with this hypothesis, the NMDA treatment, previously shown to activate AKT [30], resulted in XBP1s expression increase (Figure 5).

In apparent contrast with the present data, previous studies have reported either XBP1s mRNA overexpression or no change in SMA MNs derived from hiPSCs [23, 24]. These apparent discrepancies may stem from the preparation and use of different MN subtypes. Both previous studies analysed selected cell populations (by FACS for Ng and colleagues [23] and by gradient for Rizzo and colleagues [24]), whereas we used no cell selection in our study. Moreover, in contrast to both other studies, our protocol rapidly and efficiently provides mature spinal MNs [25], which may behave differently than immature MNs, as has been demonstrated for dopaminergic neurons [53]. Finally, we provide here the first results on UPR at the protein level in hiPSC-derived MNs, allowing us to compare IRE1 $\alpha$  activation pattern, on the one hand, and XBP1s expression, on the other. These results unquestionably revealed the defect in XBP1s expression. Of note, SMN expression rescue in the hiPSC-derived MNs resulted in XBP1s rebalancing, consistently revealing that XBP1s decrease is dependant on SMN expression.

Importantly, we report here that ATF6 activation by the small molecule AA147 in severe SMA-like mice resulted in an increase in XBP1s, its targets BiP/GRP78, and SMN expression, along with spinal MNs protection and motor behaviour improvement. AA147-dependent ATF6 activation is likely to transactivate its target gene XBP1 [20, 46], leading to increased amounts of XBP1u mRNA for IRE1 $\alpha$ , which will ultimately result in SMN expression increase and MN protection.

Ng and colleagues have indicated that Guanabenz, an inhibitor of general translation [54, 55], lessens apoptosis in SMA mouse spinal cord [23]. In fact, Guanabenz inhibits the dephosphorylation of eIF2 $\alpha$  [54]. The enhancement of eIF2 $\alpha$  phosphorylation inhibits general translation but also increases ATF4 translation [56]. Interestingly, Guanabenz has been previously shown to induce neuroprotection through ATF4 activation in a cellular model of Parkinson's disease [56]. Moreover, PERK/ATF4 pathway activation has been shown connected with other UPR branches, notably the IRE1 $\alpha$ /XBP1 pathway. Yet, PERK/ATF4 pathway activation can stimulate IRE1 $\alpha$  expression

[57] and stabilise XBP1s mRNA [58], both events leading to an increase in XBP1s expression. Finally, the results from Ng and colleagues [23] and the present results concur at considering the IRE1 $\alpha$ /XBP1 branch of the UPR as an important pathway in SMA pathogenesis, whose re-activation could elicit neuroprotective effects on SMA MNs.

In the context of available FDA-approved therapies in SMA, drugs that promote the inclusion of exon-7 in SMN pre-messenger RNA generated by SMN2 gene expression, such as Antisense Oligonucleotides [4–6] or Ridisplam [7], might be maximise by a combinational therapy that increases the substrate of these drugs, that is, SMN pre-messenger RNA, notably in severe type of SMA. This is precisely what we report here with the AA147 treatment strongly suggesting that UPR rebalancing drugs should be considered as a combinational therapy to alleviate SMA symptoms in patients.

#### ACKNOWLEDGEMENTS

The authors wish to thank Claire Mader and her team (Animal facility, BioMedTech Facilities, CNRS UMS 2009, INSERM US 36) for taking care of all the mice used in this study, S. Lefebvre for the kind gift of immortalised fibroblasts, J. Coté (University of Ottawa, Canada) for the kind gift MN-1 cells and S. Nedelec for the kind gift pEF1aFlagbiotagSMN-PGKpuro. We also thank the *Cyto2BM Molecular Biology Platform* of BioMedTech Facilities. C.B. is the recipient of a CIFRE fellowship with Biophytis company.

#### CONFLICT OF INTEREST

The authors declare that they have no competing interests.

#### AUTHOR CONTRIBUTIONS

DD designed and performed experiments, analysed data and wrote the manuscript. OB designed and analysed the IF data and ZC contributed to MN quantification. CJ, CM and LW produced and contributed to the analysis of hiPSC-derived MNs. CB, MEK and LH contributed to mouse experiments. DS contributed to RT-qPCR experiments. BDG contributed with expert advice and input on design and analysis in cloning. ChM and TJ contributed to the molecular analysis design. VKS contributed to the data analysis and to the writing of the manuscript. FC conceptualised the project and LW and FC designed the overall research, analysed the data and wrote the manuscript. All authors read and approved the final manuscript.

#### ETHICS STATEMENT

For human iPSC, experimental protocols were approved by the French Ministry of health: A02599-48. The care and treatment of animals followed the national authority (French Ministry of Research and Technology) guidelines for the detention, use and ethical treatment of laboratory animals.

#### PEER REVIEW

The peer review history for this article is available at <https://publons.com/publon/10.1111/nan.12816>.

## DATA AVAILABILITY STATEMENT

The data that support the findings of this study are available from the corresponding author upon reasonable request.

## ORCID

Cécile Martinat  <https://orcid.org/0000-0002-5234-1064>

Laure Weill  <https://orcid.org/0000-0003-3579-6582>

## REFERENCES

- Lefebvre S, Bürglen L, Reboullet S, Clermont O, Burlet P, Viollet L, Benichou B, Cruaud C, Millasseau P, Zeviani M, le Paslier D, Frézal J, Cohen D, Weissenbach J, Munnich A, Melki J Identification and characterization of a spinal muscular atrophy-determining gene. *Cell* 1995;80:155–165. doi:10.1016/0092-8674(95)90460-3, 1
- Crawford TO, Pardo CA. The neurobiology of childhood spinal muscular atrophy. *Neurobiol Dis* 1996;3:97–110. doi:10.1006/nbdi.1996.0010, 2
- Lorson CL, Androphy EJ. An exonic enhancer is required for inclusion of an essential exon in the SMA-determining gene SMN. *Hum Mol Genet* 2000;9:259–265. doi:10.1093/hmg/9.2.259, 2
- Chiriboga CA, Swoboda KJ, Darras BT, Iannaccone ST, Montes J, De Vivo DC, Norris DA, Bennett CF, Bishop KM Results from a phase 1 study of nusinersen (ISIS-SMN [Rx]) in children with spinal muscular atrophy. *Neurology* 2016;86:890–897. 10 doi:10.1212/WNL.0000000000002445
- Finkel RS, Chiriboga CA, Vajsar J, Day JW, Montes J, De Vivo DC, Yamashita M, Rigo F, Hung G, Schneider E, Norris DA, Xia S, Bennett CF, Bishop KM Treatment of infantile-onset spinal muscular atrophy with nusinersen: a phase 2, open-label, dose-escalation study. *Lancet Lond Engl* 2016;388:3017–3026. 10063 doi:10.1016/S0140-6736(16)31408-8
- Mercuri E, Darras BT, Chiriboga CA, Day JW, Campbell C, Connolly AM, Iannaccone ST, Kirschner J, Kuntz NL, Saito K, Shieh PB, Tulinius M, Mazzone ES, Montes J, Bishop KM, Yang Q, Foster R, Gheuens S, Bennett CF, Farwell W, Schneider E, de Vivo DC, Finkel RS Nusinersen versus sham control in later-onset spinal muscular atrophy. *N Engl J Med* 2018;378:625–635. 7 doi:10.1056/NEJMoa1710504
- D. S. Risdipam: First approval. *Drugs* 2020. 80, 17, 1853, 1858, doi:10.1007/s40265-020-01410-z.
- Mendell JR, Al-Zaidy S, Shell R, Arnold WD, Rodino-Klapac LR, Prior TW, Lowes L, Alfano L., Berry K., Church K., Kissel J.T., Nagendran S., Lltalien J., Sproule D.M., Wells C., Cardenas J.A., Heitzer M.D., Kaspar A., Corcoran S., Braun L., Likhite S., Miranda C., Meyer K., Foust K.D., Burghes A.H.M., Kaspar B.K. Single-dose gene-replacement therapy for spinal muscular atrophy. *N Engl J Med* 2017; 377:1713–1722. 18 doi:10.1056/NEJMoa1706198
- De Vivo DC, Bertini E, Swoboda KJ, Hwu W-L, Crawford TO, Finkel RS, de Vivo DC, Hwu WL, Kirschner J, Kuntz NL, Parsons JA, Ryan MM, Butterfield RJ, Topaloglu H, Ben-Omran T, Sansone VA, Jong YJ, Shu F, Staropoli JF, Kerr D, Sandrock AW, Stebbins C, Petrillo M, Braley G, Johnson K, Foster R, Gheuens S, Bhan I, Reyna SP, Fradette S, Farwell W Nusinersen initiated in infants during the presymptomatic stage of spinal muscular atrophy: *Interim Efficacy and Safety Results from the Phase 2 NURTURE Study Neuromuscul Disord* 2019;29:842–856. 11 doi:10.1016/j.nmd.2019.09.007
- Hensel N, Kubinski S, Claus P. The need for SMN-independent treatments of spinal muscular atrophy (SMA) to complement SMN-enhancing drugs. *Front Neurol* 2020;11:45. doi:10.3389/fneur.2020.00045
- Wadman RI, van der Pol WL, Bosboom WM, Asselman F-L, van den Berg LH, Iannaccone ST, van der Pol WL, van den Berg LH, Vrancken AFJE, Cochrane Neuromuscular Group. Drug treatment for spinal muscular atrophy type I. *Cochrane Database Syst Rev* 2019. doi:10.1002/14651858.CD006281.pub5., 12, CD006281
- Finkel RS, Mercuri E, Darras BT, Connolly AM, Kuntz NL, Kirschner J, Chiriboga CA, Saito K, Servais L, Tizzano E, Topaloglu H, Tulinius M, Montes J, Glanzman AM, Bishop K, Zhong ZJ, Gheuens S, Bennett CF, Schneider E, Farwell W, de Vivo DC Nusinersen versus sham control in infantile-onset spinal muscular atrophy. *N Engl J Med* 2017;377:1723–1732. 18 doi:10.1056/NEJMoa1702752
- Kruzik A, Fetahagic D, Hartlieb B, Dorn S, Koppensteiner H, Horling FM, Scheifflinger F, Reipert BM, de la Rosa M Prevalence of anti-adenovirus-associated Virus immune responses in international cohorts of healthy donors. *Mol Ther - Methods Clin Dev.* 2019;14: 126–133. doi:10.1016/j.omtm.2019.05.014
- Biondi O, Grondard C, Lécolle S, Deforges S, Pariset C, Lopes P, Lecolle S, Cifuentes-Diaz C, Li H, della Gaspera B, Chanoine C, Charbonnier F Exercise-induced activation of NMDA receptor promotes motor unit development and survival in a type 2 spinal muscular atrophy model mouse. *J Neurosci off J Soc Neurosci* 2008;28: 953–962. 4 doi:10.1523/JNEUROSCI.3237-07.2008
- Biondi O, Branchu J, Sanchez G, Lancelin C, Deforges S, Lopes P, Pariset C, Lecolle S, Cote J, Chanoine C, Charbonnier F In vivo NMDA receptor activation accelerates motor unit maturation, protects spinal motor neurons, and enhances SMN2 gene expression in severe spinal muscular atrophy mice. *J Neurosci off J Soc Neurosci.* 2010;30:11288–11299. 34 doi:10.1523/JNEUROSCI.1764-10.2010
- Huang S, Xing Y, Liu Y. Emerging roles for the ER stress sensor IRE1 $\alpha$  in metabolic regulation and disease. *J Biol Chem* 2019;294:18726–18741. 49 doi:10.1074/jbc.REV119.007036
- Hetz C. The unfolded protein response: controlling cell fate decisions under ER stress and beyond. *Nat rev Mol Cell Biol* 2012;13:89–102, 2, doi:10.1038/nrm3270.
- Oikawa D, Kimata Y, Kohno K, Iwakawa T. Activation of mammalian IRE1 $\alpha$  upon ER stress depends on dissociation of BiP rather than on direct interaction with unfolded proteins. *Exp Cell Res* 2009;315: 2496–2504. 15 doi:10.1016/j.yexcr.2009.06.009
- Harding HP, Zhang Y, Ron D. Protein translation and folding are coupled by an endoplasmic-reticulum-resident kinase. *Nature* 1999; 397:271–274. 6716 doi:10.1038/16729
- Yoshida H, Matsui T, Yamamoto A, Okada T, Mori K. XBP1 mRNA is induced by ATF6 and spliced by IRE1 in response to ER stress to produce a highly active transcription factor. *Cell* 2001;107:881–891, 7, doi:10.1016/S0092-8674(01)00611-0.
- Hollien J, Lin JH, Li H, Stevens N, Walter P, Weissman JS. Regulated Ire1-dependent decay of messenger RNAs in mammalian cells. *J Cell Biol* 2009;186:323–331. doi:10.1083/jcb.200903014, 3
- Sano R, Reed JC. ER stress-induced cell death mechanisms. *Biochim Biophys Acta* 2013; 12 3460 3470 doi:10.1016/j.bbamcr.2013.06.028, 1833
- Ng S-Y, Soh BS, Rodriguez-Muela N, Hendrickson DG, Price F, Rinn JL, Rubin LL Genome-wide RNA-Seq of human motor neurons implicates selective ER stress activation in spinal muscular atrophy. *Cell Stem Cell* 2015;17:569–584. doi:10.1016/j.stem.2015.08.003, 5
- Rizzo F, Nizzardo M, Vashist S, Molteni E, Melzi V, Taiana M, Salani S, Santonicola P, di Schiavi E, Bucchia M, Bordini A, Faravelli I, Bresolin N, Comi GP, Pozzoli U, Corti S Key role of SMN/SYNERIP and RNA-Motif 7 in spinal muscular atrophy: RNA-Seq and motif analysis of human motor neurons. *Brain* 2019;142:276–294. doi:10.1093/brain/awy330, 2
- Maury Y, Côme J, Piskrowski RA, Salah-Mohellibi N, Chevaleyre V, Peschanski M, Martinat C, Nedelec S Combinatorial analysis of developmental cues efficiently converts human pluripotent stem cells into multiple neuronal subtypes. *Nat Biotechnol* 2015;33:89–96. 1 doi:10.1038/nbt.3049

26. Hsieh-Li HM, Chang JG, Jong YJ, Wu MH, Wang NM, Tsai CH, Li H A mouse model for spinal muscular atrophy. *Nat Genet* 2000;24:66–70. 1 doi:[10.1038/71709](https://doi.org/10.1038/71709)
27. Monani UR, Sendtner M, Coovert DD, Parsons DW, Andreassi C, Le TT, et al. The human centromeric survival motor neuron gene (SMN2) rescues embryonic lethality in Smn(–/–) mice and results in a mouse with spinal muscular atrophy. *Hum Mol Genet* 2000;339:333–9. doi:[10.1093/hmg/9.3.333](https://doi.org/10.1093/hmg/9.3.333), 3
28. Towbin H, Gordon J. Immunoblotting and dot immunobinding—current status and outlook. *J Immunol Methods* 1984;72:313–340. doi:[10.1016/0022-1759\(84\)90001-2](https://doi.org/10.1016/0022-1759(84)90001-2), 2
29. Biondi O, Branchu J, Ben Salah A, Houdebine L, Bertin L, Chali F, Desseille C, Weill L, Sanchez G, Lancelin C, Aid S, Lopes P, Pariset C, Lecolle S, Cote J, Holzenberger M, Chanoine C, Massaad C, Charbonnier F IGF-1R reduction triggers neuroprotective signaling pathways in spinal muscular atrophy mice. *J Neurosci* 2015;35:12063–12079. 34 doi:[10.1523/JNEUROSCI.0608-15.2015](https://doi.org/10.1523/JNEUROSCI.0608-15.2015)
30. Branchu J, Biondi O, Chali F, Collin T, Leroy F, Mamchaoui K, Makoukji J, Pariset C, Lopes P, Massaad C, Chanoine C, Charbonnier F Shift from extracellular signal-regulated kinase to AKT/cAMP response element-binding protein pathway increases survival-motor-neuron expression in spinal-muscular-atrophy-like mice and patient cells. *J Neurosci off J Soc Neurosci*. 2013;33:4280–4294. 10 doi:[10.1523/JNEUROSCI.2728-12.2013](https://doi.org/10.1523/JNEUROSCI.2728-12.2013)
31. Livak KJ, Schmittgen TD. Analysis of relative gene expression data using real-time quantitative PCR and the 2(-Delta Delta C [T]) Method. *Methods San Diego Calif* 2001;25:402–408. doi:[10.1006/meth.2001.1262](https://doi.org/10.1006/meth.2001.1262), 4
32. Renvoisé B, Khoobarry K, Gendron M-C, Cibert C, Viollet L, Lefebvre S. Distinct domains of the spinal muscular atrophy protein SMN are required for targeting to Cajal bodies in mammalian cells. *J Cell Sci* 2006;119 4:680–692. doi:[10.1242/jcs.02782](https://doi.org/10.1242/jcs.02782)
33. Zeng L, Zampetaki A, Margariti A, Pepe AE, Alam S, Martin D, Xiao Q, Wang W, Jin ZG, Cockerill G, Mori K, Li YSJ, Hu Y, Chien S, Xu Q Sustained activation of XBP1 splicing leads to endothelial apoptosis and atherosclerosis development in response to disturbed flow. *Proc Natl Acad Sci U S A*. 2009;106:8326–8331. doi:[10.1073/pnas.0903197106](https://doi.org/10.1073/pnas.0903197106), 20
34. Bigot A, Klein AF, Gasnier E, Jacquemin V, Ravassard P, Butler-Browne G, Mouly V, Furling D Large CTG repeats trigger p16-dependent premature senescence in myotonic dystrophy type 1 muscle precursor cells. *Am J Pathol* 2009;174:1435–1442. doi:[10.2353/ajpath.2009.080560](https://doi.org/10.2353/ajpath.2009.080560), 4
35. Salazar-Gruoso EF, Kim S, Kim H. Embryonic mouse spinal cord motor neuron hybrid cells. *Neuroreport* 1991;2:505–508. 9 doi:[10.1097/00001756-199109000-00002](https://doi.org/10.1097/00001756-199109000-00002)
36. Singh NN, Hoffman S, Reddi PP, Singh RN. Spinal muscular atrophy: broad disease spectrum and sex-specific phenotypes. *Biochimica et Biophysica Acta - Molecular Basis of Disease*. 2021;
37. Kim JK, Jha NN, Feng Z, Faleiro MR, Chiriboga CA, Wei-Lapierre L, Dirksen RT, Ko CP, Monani UR Muscle-specific SMN reduction reveals motor neuron-independent disease in spinal muscular atrophy models. *J Clin Invest* 2020. doi:[10.1172/JCI131989](https://doi.org/10.1172/JCI131989), 130, 3, 1271, 1287.
38. Bae D, Moore KA, Mella JM, Hayashi SY, Hollien J. Degradation of Blos1 mRNA by IRE1 repositions lysosomes and protects cells from stress. *J Cell Biol* 2019;218:1118–1127. 4 doi:[10.1083/jcb.201809027](https://doi.org/10.1083/jcb.201809027)
39. Castro-Mondragon JA, Riudavets-Puig R, Rauluseviciute I, Berhanu Lemma R, Turchi L, Blanc-Mathieu R, Lucas J, Boddie P, Khan A, Manosalva Pérez N, Fornes O, Leung TY, Aguirre A, Hammal F, Schmelter D, Baranasic D, Ballester B, Sandelin A, Lenhard B, Vandepoele K, Wasserman WW, Parcy F, Mathelier A JASPAR 2022: the 9th release of the open-access database of transcription factor binding profiles. *Nucleic Acids Res* 2021;;gkab1113. D1 D165 D173 doi:[10.1093/nar/gkab1113](https://doi.org/10.1093/nar/gkab1113)
40. Kreft Ł, Soete A, Hulpiau P, Botzki A, Saeys Y, De Bleser P. ConTra v3: a tool to identify transcription factor binding sites across species, update 2017. *Nucleic Acids Res* 2017;45:W490–W494. W1 doi:[10.1093/nar/gkx376](https://doi.org/10.1093/nar/gkx376)
41. Cross BCS, Bond PJ, Sadowski PG, Jha BK, Zak J, Goodman JM, Silverman RH, Neubert TA, Baxendale IR, Ron D, Harding HP The molecular basis for selective inhibition of unconventional mRNA splicing by an IRE1-binding small molecule. *Proc Natl Acad Sci U S A*. 2012;109:E869–E878. 15 doi:[10.1073/pnas.1115623109](https://doi.org/10.1073/pnas.1115623109)
42. Clauss IM, Chu M, Zhao JL, Glimcher LH. The basic domain/leucine zipper protein hXBP-1 preferentially binds to and transactivates CRE-like sequences containing an ACGT core. *Nucleic Acids Res* 1996;24:1855–1864. 10 doi:[10.1093/nar/24.10.1855](https://doi.org/10.1093/nar/24.10.1855)
43. Acosta-Alvear D, Zhou Y, Blais A, Tsikitis M, Lents NH, Arias C, Lennon CJ, Kluger Y, Dynlacht BD XBP1 controls diverse cell type- and condition-specific transcriptional regulatory networks. *Mol Cell* 2007;27:53–66. 1 doi:[10.1016/j.molcel.2007.06.011](https://doi.org/10.1016/j.molcel.2007.06.011)
44. Grondard C, Biondi O, Armand A-S, Lécolle S, Della Gaspera B, Pariset C, Li H., Gallien C.L., Vidal P.P., Chanoine C., Charbonnier F. Regular exercise prolongs survival in a type 2 spinal muscular atrophy model mouse. *J Neurosci off J Soc Neurosci*. 2005;25:7615–7622. 33 doi:[10.1523/JNEUROSCI.1245-05.2005](https://doi.org/10.1523/JNEUROSCI.1245-05.2005)
45. Tsai L-K, Tsai M-S, Lin T-B, Hwu W-L, Li H. Establishing a standardized therapeutic testing protocol for spinal muscular atrophy. *Neurobiol Dis* 2006;24:286–295. doi:[10.1016/j.nbd.2006.07.004](https://doi.org/10.1016/j.nbd.2006.07.004), 2
46. Paxman R, Plate L, Blackwood EA, Glembotski C, Powers ET, Wiseman RL, Kelly JW Pharmacologic ATF6 activating compounds are metabolically activated to selectively modify endoplasmic reticulum proteins. *Elife* 2018;7:e37168. doi:[10.7554/eLife.37168](https://doi.org/10.7554/eLife.37168)
47. Reimold AM, Iwakoshi NN, Manis J, Vallabhajosyula P, Szomolanyi-Tsuda E, Gravalles EM, Friend D, Grusby MJ, Alt F, Glimcher LH Plasma cell differentiation requires the transcription factor XBP-1. *Nature* 2001;412:300–307. 6844 doi:[10.1038/35085509](https://doi.org/10.1038/35085509)
48. Lee A-H, Chu GC, Iwakoshi NN, Glimcher LH. XBP-1 is required for biogenesis of cellular secretory machinery of exocrine glands. *EMBO j* 2005;24:4368–4380. doi:[10.1038/sj.emboj.7600903](https://doi.org/10.1038/sj.emboj.7600903), 24
49. Shoulders MD, Ryno LM, Genereux JC, Moresco JJ, Tu PG, Wu C, Yates III JR, Su AI, Kelly JW, Wiseman RL Stress-independent activation of XBP1s and/or ATF6 reveals three functionally diverse ER proteostasis environments. *Cell Rep* 2013;3:1279–1292. doi:[10.1016/j.celrep.2013.03.024](https://doi.org/10.1016/j.celrep.2013.03.024), 4
50. Yamamoto K, Sato T, Matsui T, Sato M, Okada T, Yoshida H, Harada A, Mori K Transcriptional induction of mammalian ER quality control proteins is mediated by single or combined action of ATF6α and XBP1. *Dev Cell* 2007;13:365–376. doi:[10.1016/j.devcel.2007.07.018](https://doi.org/10.1016/j.devcel.2007.07.018), 3
51. Lee A-H, Heidtman K, Hotamisligil GS, Glimcher LH. Dual and opposing roles of the unfolded protein response regulated by IRE1α and XBP1 in proinsulin processing and insulin secretion. *Proc Natl Acad Sci U S A*. 2011;108:8885–8890. 21 doi:[10.1073/pnas.1105564108](https://doi.org/10.1073/pnas.1105564108)
52. Wang Y, Zhang Y, Yi P, Dong W, Nalin AP, Zhang J, Zhu Z, Chen L, Benson DM, Mundy-Bosse BL, Freud AG, Caligiuri MA, Yu J The IL-15-AKT-XBP1s signaling pathway contributes to effector functions and survival in human NK cells. *Nat Immunol* 2019;20:10–17. doi:[10.1038/s41590-018-0265-1](https://doi.org/10.1038/s41590-018-0265-1), 1
53. Valdés P, Mercado G, Vidal RL, Molina C, Parsons G, Court FA, Martínez A, Galleguillos D, Armentano D, Schneider BL, Hetz C Control of dopaminergic neuron survival by the unfolded protein response transcription factor XBP1. *Proc Natl Acad Sci U S A*. 2014; 111:6804–6809. 18 doi:[10.1073/pnas.1321845111](https://doi.org/10.1073/pnas.1321845111)
54. Tsaytler P, Harding HP, Ron D, Bertolotti A. Selective inhibition of a regulatory subunit of protein phosphatase 1 restores proteostasis. *Science* 2011;332:91–94. 6025 doi:[10.1126/science.1201396](https://doi.org/10.1126/science.1201396)

55. Pérez-Arancibia R, Rivas A, Hetz C. (off)Targeting UPR signaling: the race toward intervening ER proteostasis. *Expert Opin Ther Targets* 2018;22:97–100. doi:[10.1080/14728222.2018.1420169](https://doi.org/10.1080/14728222.2018.1420169), 2
56. Sun X, Aimé P, Dai D, Ramalingam N, Crary JF, Burke RE, Greene LA, Levy OA Guanabenz promotes neuronal survival via enhancement of ATF4 and parkin expression in models of Parkinson disease. *Exp Neurol* 2018;303:95–107. doi:[10.1016/j.expneurol.2018.01.015](https://doi.org/10.1016/j.expneurol.2018.01.015)
57. Tsuru A, Imai Y, Saito M, Kohno K. Novel mechanism of enhancing IRE1 $\alpha$ -XBP1 signalling via the PERK-ATF4 pathway. *Sci Rep* 2016;6:24217. 1 doi:[10.1038/srep24217](https://doi.org/10.1038/srep24217)
58. Majumder M, Huang C, Snider MD, Komar AA, Tanaka J, Kaufman RJ, Krokowski D, Hatzoglou M A novel feedback loop regulates the response to endoplasmic reticulum stress via the cooperation of cytoplasmic splicing and mRNA translation. *Mol Cell Biol* 2012;32:992–1003. doi:[10.1128/MCB.06665-11](https://doi.org/10.1128/MCB.06665-11), 5

## SUPPORTING INFORMATION

Additional supporting information may be found in the online version of the article at the publisher's website.

**How to cite this article:** D'Amico D, Biondi O, Januel C, et al. Activating ATF6 in spinal muscular atrophy promotes SMN expression and motor neuron survival through the IRE1 $\alpha$ -XBP1 pathway. *Neuropathol Appl Neurobiol*. 2022;48(5):e12816. doi:[10.1111/nan.12816](https://doi.org/10.1111/nan.12816)